DEVELOPMENT OF A BIOGAS COMBUSTION CFD MODEL FOR THE ANALYSIS OF TRACE EMISSIONS

Janaka Nayanajith Bandara

208018E

Degree of Master of Science

Department of Chemical and Process Engineering

University of Moratuwa

Sri Lanka

September 2021

DEVELOPMENT OF A BIOGAS COMBUSTION CFD MODEL FOR THE ANALYSIS OF TRACE EMISSIONS

Adikarinayaka Mudiyanselage Janaka Nayanajith Bandara

208018E

Thesis submitted in partial fulfilment of the requirements for the degree Master of Science (Major Component of Research)

Department of Chemical and Process Engineering

University of Moratuwa

Sri Lanka

September 2021

DECLARATION

I declare that this is my own work and this thesis/dissertation2 does not incorporate without acknowledgement any material previously submitted for a Degree or Diploma in any other University or institute of higher learning and to the best of my knowledge and belief it does not contain any material previously published or written by another person except where the acknowledgement is made in the text.

Also, I hereby grant to University of Moratuwa the non-exclusive right to reproduce and distribute my thesis/dissertation, in whole or in part in print, electronic or other medium. I retain the right to use this content in whole or part in future works (such as articles or books).

Signature: ……..…… Date: ……

Declaration (Supervisor)

The above candidate has carried out research for the Masters/MPhil/PhD thesis/ dissertation under my supervision.

Signature of the Supervisor: …… Date: …….

Prof. Mahinsasa Narayana

Professor

Department of Chemical & Process Engineering

University of Moratuwa

Signature of the Co-Supervisor: …… Date: ……..

Prof. Christoph Bayer,

Technische Hochschule Nürnberg Georg Simon Ohm,

Nürnberg, Germany.

TABLE OF CONTENTS

LIST OF FIGURES

LIST OF TABLES

LIST OF APPENDICES

NOMENCLATURE

A/F	Air to fuel ratio
$(A/F)_{stoic}$	Air to fuel ratio in the stoichiometric mixture
λ	Equivalent ratio
$\dot{Q}$	Rate of heat transfer
$\dot{W}$	Power
h	Enthalpy
v	Velocity
g	Acceleration of gravity
$\dot{m}$	Mass flowrate
z	Elevation
ρ	Density
Y_i	Mass fraction of specie 'i' in the control volume
u_j	Velocity
D_i	Diffusion coefficient
R_i	Reaction source term
$M_{w,i}$	Molecular weight of specie 'i'
$\hat{R}_{i,r}$	Molar rate of creation/destruction of specie 'i' in reaction 'r'
N_R	Number of reactions
N_r	Number of chemical species in reaction 'r'
$C_{j,r}$	Molar concentration of specie 'j' in reaction 'r'
$\eta'_{j,r}$	Forward rate exponent
$\eta''_{j,r}$	Backward rate exponent
$k_{f,r}$	Rate constant
A_r	Pre-exponential factor of reaction 'r'
E_r	Activation energy for the reaction 'r'
R	Universal gas constant
T	Absolute temperature
E	Total energy
p	Pressure
q	Heat flux vector
τ	Viscous stress tensor
g	Gravitational constant
r	Total heat released/absorbed by reactions
u	Wind speed
u_r	Known wind speed at reference height
z_r	Reference height
ν	Kinematic viscosity
F	Sum of body forces (gravity)
F_c	Coriolis force
T_0	Reference temperature
β	Coefficient of thermal expansion
m	Mass
ω	Angular velocity of the earth
V	Tangential velocity
φ	Latitude of the location

ABSTRACT

Biogas is emitted from landfills, anaerobic digesters, and many other biomass sources. Emitted biogas is usually burnt in order to reduce greenhouse effect and to get energy. Burning of biogas emits several pollutants, mainly CO_2, NO_x and SO_2. Reducing the of emissions is very important in combustion. Emissions of combustion can be analysed experimentally or by computer simulations. Experiments are very accurate and expensive. Computer simulation is an economic way of analysing combustion systems. In this study emissions of biogas combustion are analysed with computer simulations.

There are several methods of reducing emissions in combustion such as excess air control, air staging, fuel Staging, flue gas recirculation etc. In this study, the effect of excess air in biogas combustion is analysed. The range of optimum equivalent ratio was found as 0.85-1.1.

Emitted gasses get dissipated in the atmosphere with the wind. The environmental effect from emissions of a 20kW industrial biogas burner in Colombo area was analysed using CFD simulations. Results show that the ground level is below environmental standard limits.

Keywords: Biogas, Combustion, Equivalent Ratio, CFD, Atmospheric dispersion

ACKNOWLEDGEMENTS

I am thankful to my supervisor Prof. Mahinsasa Narayana and co-supervisor Prof. Christoph Bayer for their encouragement, guidance, and time throughout my study. I should thank Dr. Niranjan Fernando for the guidance given on CFD modelling. I am also thankful to Prof. S. Walpalage, Head of the Department of Chemical & Process Engineering and Prof. A.A.P. de Alwis, Dean, Faculty of Graduate Studies, University of Moratuwa for enrolling me for the M.Sc. degree. I am thankful for National Research Council of Sri Lanka for the financial support and Europe Sri Lanka Capacity Building in Energy Circular Economy "EUSL-Energy" project for equipment grant. Finally, I should thank my parents, staff of University of Moratuwa and my colleagues as well for their supports.

1. INTRODUCTION

Industries generate several types of waste, and they must be treated before releasing to the environment. Most of the generated waste is organic waste. Anaerobic digestion [1] is a main method of treating organic waste. Biogas is produced as a by-product in anaerobic digestion. Biogas is generated in landfills too [2].

Biogas is a mixture of methane, carbon dioxide, small amounts of nitrogen, oxygen, hydrogen sulphide, and some other gases. It must be carefully handled, and it cannot be directly released to the environment due to Methane's global warming potential of 23 [3]. Hence, produced biogas is burnt in a flare or in a combustion chamber. Although complete combustion should release only CO_2 and H_2O, in practice carbon monoxide (CO), carbon dioxide (CO_2), oxides of nitrogen (NOx), volatile organic compounds (VOCs), trace amounts of Sulphur dioxide (SO_2), particulate matter (PM) and unburned fuel can be released. These emissions depend on air/fuel ratio (A/F), temperature, and mixing properties in the combustion chamber. When the A/F ratio is lower, it releases unburned fuel and CO, and when the A/F is higher it releases less CO, and reduces the flame temperature. If air is used instead of pure oxygen, N_2 in the air will be converted into NOx. Trace amounts of NH_3 in fuel is also converted to NO_x in the combustion process. Therefore, optimum A/F should be maintained with perfect mixing to achieve high temperatures with low CO and NOx emission.

NO_x poses a threat to the environment due to formation of photochemical smog, formation of ground level ozone [4], acid rain etc. [5] and health risks [6]. Therefore, NOx emission control is very important in combustion. There are several NOx emission control methods in combustion such as excess air control, air staging, flue gas recirculation, fuel staging etc. Excess air control, which is the simplest method, is analysed in this study.

The combustion system should be analysed experimentally or by computer simulations. Experimental analyses are expensive and computer simulations are economical. Therefore, usually analysis with computational simulation is done first and then the results are finetuned with physical experiments. Excess air control in a small-scale combustion chamber is analysed with computational simulations in this

study. Computational Fluid Dynamics model (CFD) for the combustion system was developed. The CFD model was validated using DLR $CH_4/H_2/N_2$ flame [7].

When designing an industrial equipment, initial experiments are done in small-scale equipment. Then the equipment is scaled up to the industrial scale. In this study excess air control in a small-scale combustion chamber is analysed using the validated CFD model. Then, the dispersion of emissions from a similar industrial scale combustor is analysed.

Emitted NO_x spreads over the atmosphere. Spreading direction and dissipation rate depends on the wind velocity and exhaust temperature of the chimney. During the designing of a combustion system, NO_x formation and dissipation must be analysed in order to confirm that all the environmental standards are met. In this study, combustion of biogas was analysed and stack emission to the environment was estimated with a NO_x and SO_2 dispersion model in flat terrain by Computational Fluid Dynamics model (CFD).

1.1. Objective

- Development and validation of a CFD model to analyse biogas combustion by available chemical kinetics.
- Optimization of process parameters to obtain minimum pollutant in the emission using the developed model
- Analysis of dissipation of emissions in the atmosphere

1.2. Methodology

First existing emission control methods used in combustion were studied. The simplest method of controlling emissions from combustors was found as excess air control. That was selected as the emission control method for this study.

CFD simulation is an achievable way of analysing a combustion system. Therefore, the considered system was analysed with CFD simulations in this study. Mathematical model was developed for heat and mass transfer and reactions. The turbulence models available are direct numerical simulation (DNS), Large Eddy Simulation (LES) and

Reynolds Averaged Navier-Stokes (RANS). RANS needs the least computational power and DNS needs the highest computational power. Researchers proved that RANS can accurately simulate biogas combustion and it was further validated using experimental data of DLR flame. GRIMech, which is an accepted reaction mechanism for biogas combustion, was used in this study for simulation of combustion after further validation with DLR flame.

Effect of excess air to emissions of biogas combustion was analysed considering a small-scale combustion chamber. The combustion chamber was simulated using the validated CFD solver. Based on simulation results, the optimum equivalent ratio for the considered system was defined.

The effect of emissions depends on emission quantity as well as dispersion of emissions in the atmosphere. Therefore, the dispersion of emissions in the atmosphere was analysed. Smagorinsky LES model is the recommended CFD model for atmospheric simulations. It was further validated by comparing with published experimental data. Emissions from a 20kW industrial burner in Colombo area was simulated and analysed the health and environmental effects.

1.3. Industrial waste treatment

Industries generate different types of wastes such as organic waste, heavy metals, hazardous chemicals, radioactive materials, particulate matter, greenhouse gasses, toxic gasses etc. Most of the wastes are organic waste and usually dissolved in water. The industry must treat these wastes before releasing them to the environment. The most common method of treating organic wastes is aerobic and anaerobic digestion. Aerobic digestion does not generate any useful by-product. But anaerobic digestion generates biogas as a by-product.

1.4. Biogas generation

Biogas is a renewable fuel produced by the decomposition of organic matter such as food and animal waste [8]. Methane is the main combustible substance in biogas. When organic matter is digested by microorganisms in anaerobic environment, biogas

is produced as a by-product. The bacteria which produce methane in biogas are called Methanogens.

There are many sources of biogas. Some of the main raw materials of generating biogas are:

- Livestock waste
- Landfill gas
- Industrial wastewater

Livestock Waste

Livestock wastes constitute the most used substrate for biogas generation. Manure from poultry, cattle, and pigs are all good examples of this waste. Livestock wastes naturally contains sufficient amounts of Methanogens.

Landfill Gas

Municipal solid waste landfills are the third-largest source of human-related methane emissions in many countries. Landfills produce methane by decomposing organic matter by Methanogens in soil or waste.

Industrial wastewater

Industrial wastewater contains a huge amount of organic matter. They do a huge damage to the environment if discharged without necessary treatments. Burning, chemical treatment, aerobic digestion and anaerobic digestion are the main methods of treating organic wastes. The treatment method is decided based on the ingredients and the content of the waste. The waste treatment process may have several steps with different treatment methods. When they are treated in an anaerobic digester, biogas is produced as a by-product. Biogas has an average global warming potential of 21, which is very high. Therefore, it should not be released to the atmosphere. Usually, generated biogas is used as an energy source in the same industry or burned in a flare. It may be released to the environment without burning if the amount of biogas produced is very low.

1.5. Applications of Biogas Combustion

Biogas is used for several purposes:

- Domestic cooking
- House heating
- Generation of electricity using engines
- Industrial boilers

Most of the industries that produce biogas in waste treatment process use that to generate electricity or to fulfil heating requirements of the industry. Some of the industries burn biogas in a flare without using effectively.

1.6. Biogas Composition

Table 1: Composition of Biogas

Component	% Volume
CH_4	60-75
CO_2	19-33
N_2	1
O_2	0-5
H_2O	6
H_2S	1000-4000 ppm
NH_3	50-100ppm

Source: Biogas composition [9]

1.7. Emissions of Biogas combustion

Table 2 presents emission compositions of biogas combustion which are calculated based on composition of biogas.

Table 2: Emissions of Biogas combustion

Component	Average Composition	Global warming potential	Major Environmental Impact
CO_2	12 %v/v	1	Global warming

H_2O	15 %v/v	-	Negligible
N_2	70 %v/v	0	Negligible
O_2	3 %v/v	0	Negligible
SO_2	50ppm	0	Acid rains
NO_x	up to50ppm	0	Photochemical smog Acid rain Make ground level ozone Harmful for lungs
CO	Depend on efficiency	0	Toxic
Unburnt CH_4	Depend on efficiency	21	Global warming

Methane

Methane is a severe greenhouse gas. Therefore, emission of CH_4 should be minimized. Burning of CH_4 is the usual practice in the industry to reduce CH_4 emission.

Carbon dioxide

CO_2 is a greenhouse gas. But its greenhouse effect is less than CH_4. Therefore, burning of CH_4 in order to reduce greenhouse gas emission is generally accepted.

Sulphur dioxide

SO_2 is the main reason for acid rains. SO_2 should be reduced by absorbing from flue gas or by removing Sulphur from fuel.

NO_x

Biomass combustion systems emit nitrogen oxides which should be reduced since they contribute to the formation of acid rain and photochemical smog and to produce ground level ozone. The NOx emissions from biomass combustion are mainly caused by the nitrogen in the fuel. High temperature combustion produces thermal NOx.

1.8. NO Formation Mechanisms

In the combustion process Nitrogen in fuel and air is first converted into NO and then converted to NO_2. There are three main NO formation mechanisms in combustion [10].

i. Thermal NO mechanism
ii. Prompt NO mechanism
iii. Fuel NO_x

Formed NO is converted to NO_2 in the atmosphere as NO is an unstable substance.

Thermal NO mechanism

High temperature converts O_2 into oxygen atoms. As atomic oxygen is highly reactive, it forms NO with available N_2 according to the below mechanism. The reaction rate is very high above 1800K temperature.

$$O + N_2 \leftrightarrow NO + N \tag{1.1}$$

$$N + O_2 \leftrightarrow NO + O \tag{1.2}$$

$$N + OH \leftrightarrow NO + H \tag{1.3}$$

Steady state NO formation rate is expressed as in equation (1.4) [10]

$$\frac{d(NO)}{dt} = 2k_1(O)(N_2) = 1.70 \times 10^{17} T^{-\frac{1}{2}} e^{\frac{-69750}{T(K)}} (O_2)_{eq}^{\frac{1}{2}} (N_2)_{eq}\ mol/cm^3 s \tag{1.4}$$

The thermal NO formation rate will be reduced when the availability of oxygen, nitrogen or flame temperature is decreased.

Prompt NO mechanism

The presence of a second mechanism leading to NO_x formation was first proposed by Charles Fenimore [11] and was termed "prompt NO_x" in 1971. When thermal and fuel NO_x are eliminated, some NO_x formation was still observed. Fenimore attributed this to the reaction of atmospheric nitrogen with combustion radicals occurring in the earliest stages of combustion.

$$CH^- + N_2 \rightarrow HCN + N^- \quad (1.5)$$

$$N^- + OH \rightarrow NO + H^- \quad (1.6)$$

$$N^- + O_2 \rightarrow NO + O^- \quad (1.7)$$

$$HCN + O_2 \rightarrow NO + CO + H^- \quad (1.8)$$

Because this mechanism is not significantly temperature dependent, it becomes more important when other NO_x formation mechanisms have been suppressed. Reducing of prompt NO_x formation is very difficult. Therefore, prompt NO_x must be lived with, and focus is normally placed on suppressing the other two main NO_x mechanisms.

Fuel NO_x

When fuel has chemically bonded nitrogen, it is oxidized to NO_x during combustion. Nitrogen is usually removed from fossil fuels in the refining process. Biogas contains a trace amount of ammonia which is converted to NO and water during combustion.

$$4NH_3 + 5O_2 \rightarrow 4NO + 6H_2O \quad (1.9)$$

Fuel NO formation mechanism is not considered in this study as it is very low compared to other two mechanisms

1.9. NO formation control methods

There are many methods of reducing emissions [12]. Main methods are

- Excess air control
- Air staging (overfire air or two-stage combustion)
- Flue gas recirculation
- Fuel staging (burner out of service, fuel biasing, reburning or three stage combustion)

Excess air control

Complete combustion cannot be achieved by suppling air in the stoichiometric ratio. Therefore, excess air must be provided to achieve complete combustion. According to

thermal NO mechanism, rate of NO formation depends on available nitrogen concentration. Therefore, excess air must be controlled at the minimum level to achieve complete combustion with least NOx emission.

[13] explains a tuning method to minimize emissions of a gas turbine.

Air staging

Air staging is a method used to reduce NO_x emissions from fuel nitrogen. When there is less oxygen available in the reaction zone, fuel nitrogen is converted to N_2 instead of NO. Therefore, less air is provided to the primary stage as shown in Figure 1.

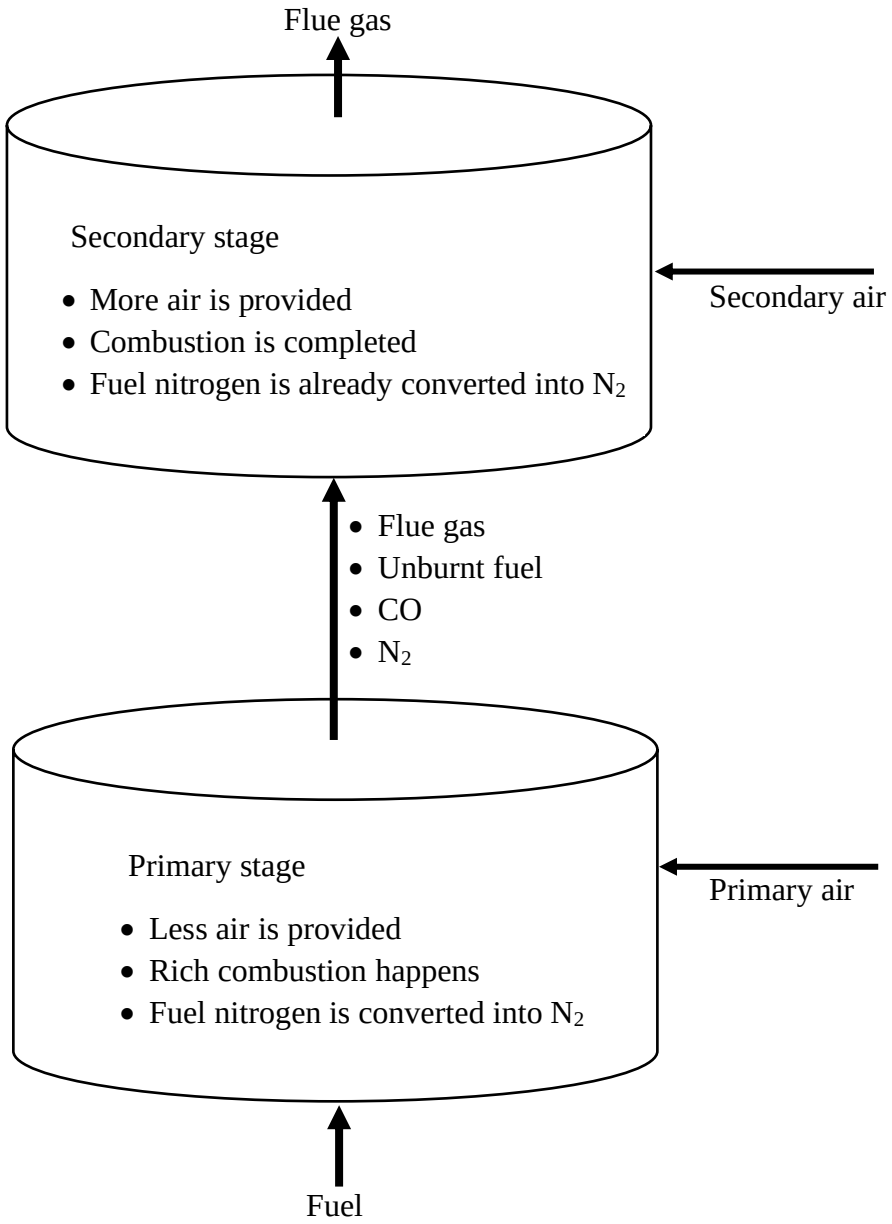

Figure 1: Air staging

Then additional air is provided to the secondary stage to complete the combustion

[14] shows that rich combustion with high temperature in primary zone reduces NOx emissions,

Fuel Staging

Usually there are three stages in fuel staging.

1. Primary combustion zone
2. Reburn zone
3. Burnout zone

The fuel which has nitrogen is fed to the stage 1. As rich combustion is happening, most of the fuel nitrogen will be converted in to N_2. However, some amount of fuel nitrogen is converted into NO also.

In the second stage produced NO is converted into N_2 by hydrocarbon radicals and produced CO.

Stage 3 completes the combustion with excess air.

[15] shows that fuel staging is good for fuels with high nitrogen content.

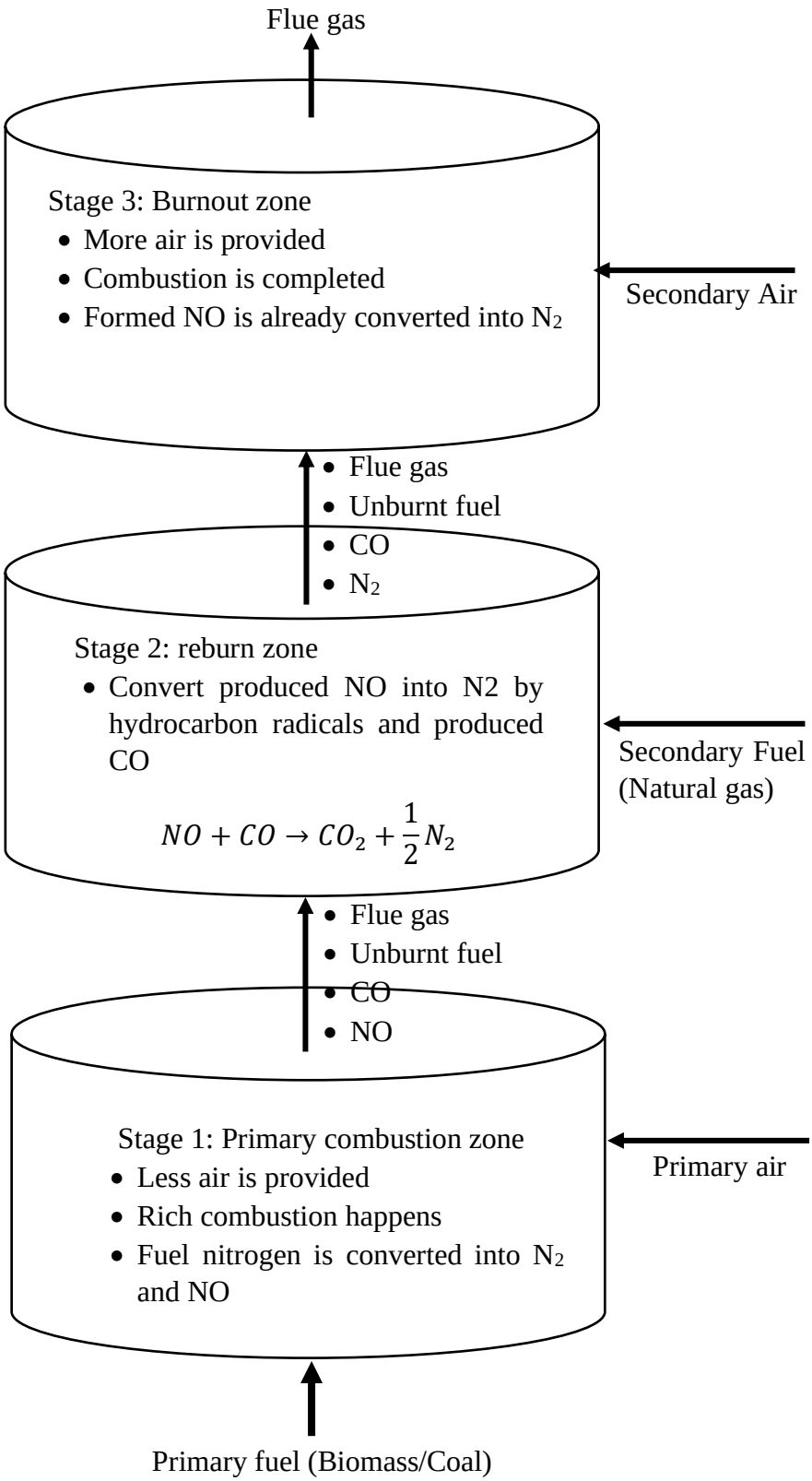

Figure 2: Fuel Staging

Flue gas recirculation

Flue Gas Recirculation (FGR) is the process of taking a portion of the flue gas from a combustion process and recirculating it back through combustor. When the process is used in internal combustion engines it is commonly referred to as exhaust gas recirculation (EGR). EGR for internal combustion engines, was introduced in the 1970s. EGR is now required by the United States Environmental Protection Agency for diesel engines, in order to decrease NO_x emissions.

FGR reduces thermal NO_x by reducing the flame temperature by diluting the fuel-air mix with inert gases like N_2, H_2O and CO_2. The lower temperature prevents diatomic nitrogen and oxygen in the fuel-air mix from reacting. FGR is not effective in reducing fuel NO_x.

Figure 3 shows that properly maintaining flue gas recirculation reduces NOx without increasing CO [16]. That explains that the increasing of FGR ratio reduces NOx as the graph in Figure 3.

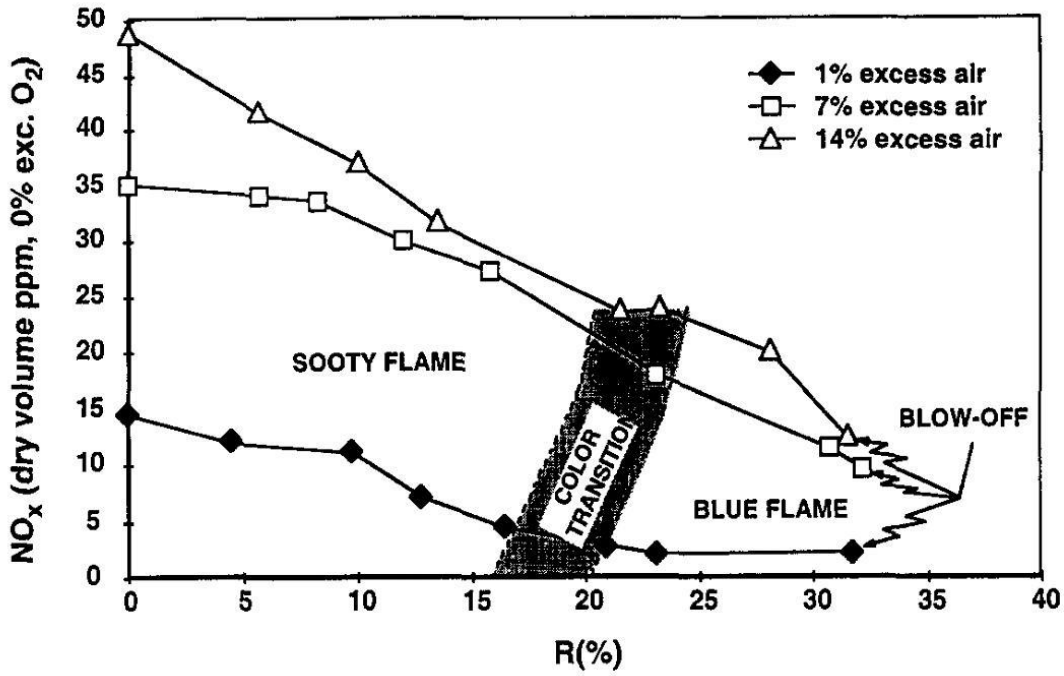

Figure 3: Effect of FGR ratio

Source: Flue gas recirculation in a gas-fired laboratory furnace [16]

Applicability of each emission control method

Table 3: Applicability of different emission control method

Excess air control	Can be applied to any system
Air staging	Implemented where fuel contains N
Fuel staging	Implemented when primary fuel contains N
Flue gas recirculation	Implemented when a higher flowrate is needed

1.10. Experimental combustion analysis

Emissions

The most accurate method of analysing a combustion system is using experimental data. An apparatus as Figure 4 can be used to analyse emissions of an engine [17].

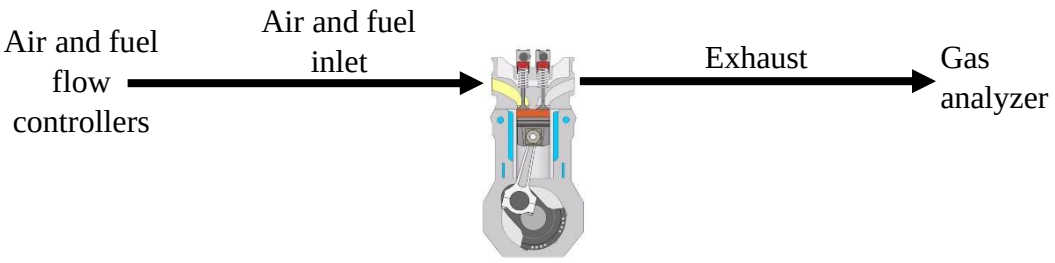

Figure 4: Engine exhaust analyse experimental setup

Emissions of any combustion system can be measured using a similar method.

Flame propagation speed

Flame propagation speed is a very important parameter in combustion, especially in internal engines. An apparatus as in Figure 5 is used for such experiments [18].

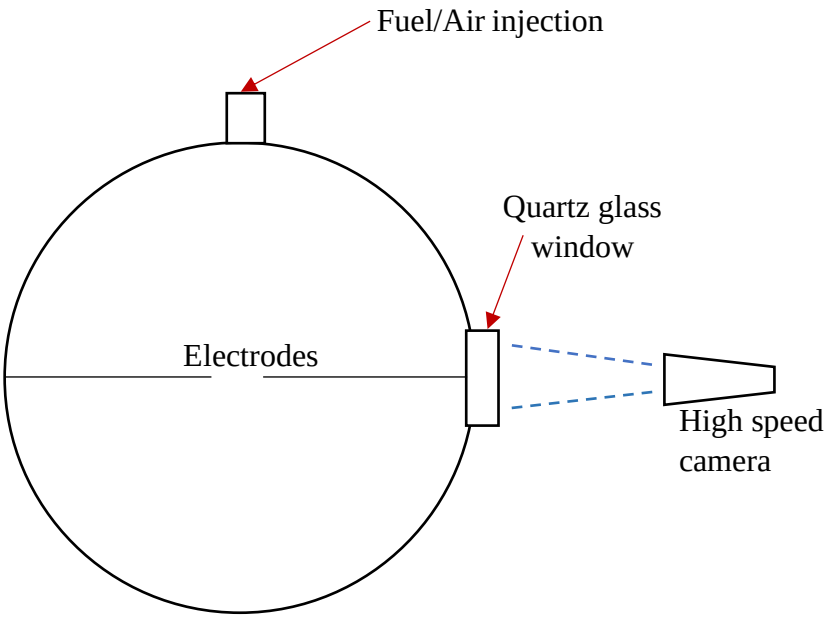

Figure 5: Experimental setup of flame propagation speed

Flame profile

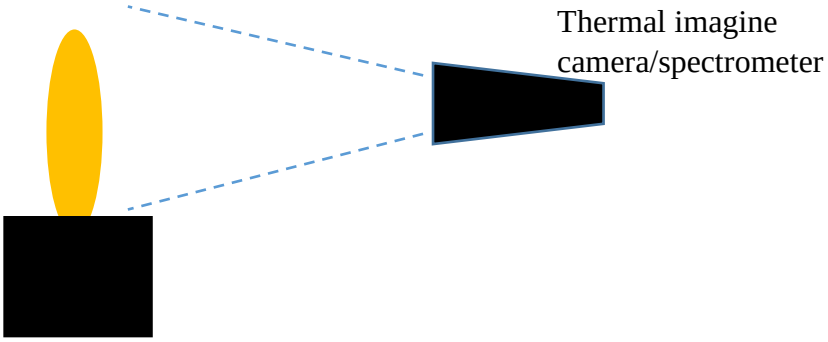

Figure 6: Experimental setup to identify flame profile

Thermal imaging camera is used to obtain the temperature profile. A spectrometer is used to get species profile in the flame [19].

1.11. Analysis of combustion process

Temperature and emissions of combustion are very important in applications. High temperature flame is required in industrial applications. Emissions are a large threat to the environment and health. Combustors must be optimized to get maximum temperature with less emissions. Combustion process should be properly analysed to design and maintain combustors with optimum operating conditions.

Experimental analysis is done to analyse combustion processes more accurately. Temperature and specie profiles of the flame can be experimentally obtained using thermal imaging cameras and spectrometers. Emissions are analysed using Gas chromatography–mass spectrometry. Gas combustors as well as these analytical instruments are very expensive. If different combustors are analysed, there must be each combustor available in the experiment lab which may not be economically feasible.

Computer simulation is an economical way of analysing combustion systems. First a mathematical model of the system should be developed to run a computational simulation. The model must be validated by comparing with some experimental data before using for analysis. Knowledge on science, mathematical modelling and computer programming is needed for computer simulator development. Huge computational power is required to run complex simulations. A 32 core 64 thread 2GHz processor was used in this study. Even though required expertise knowledge and computer processing power is expensive, it is more economical than physical experiments because knowledge and high-performance computers are available nowadays in many research institutes. Researchers recommend to first analyse the combustion process with computer simulations and then fine-tune the results with physical experiments. This study is done to analyse the effect of excess air in a biogas combustion chamber and the atmospheric dispersion of emissions from an industrial burner.

1.11.1. A/F emission analysis

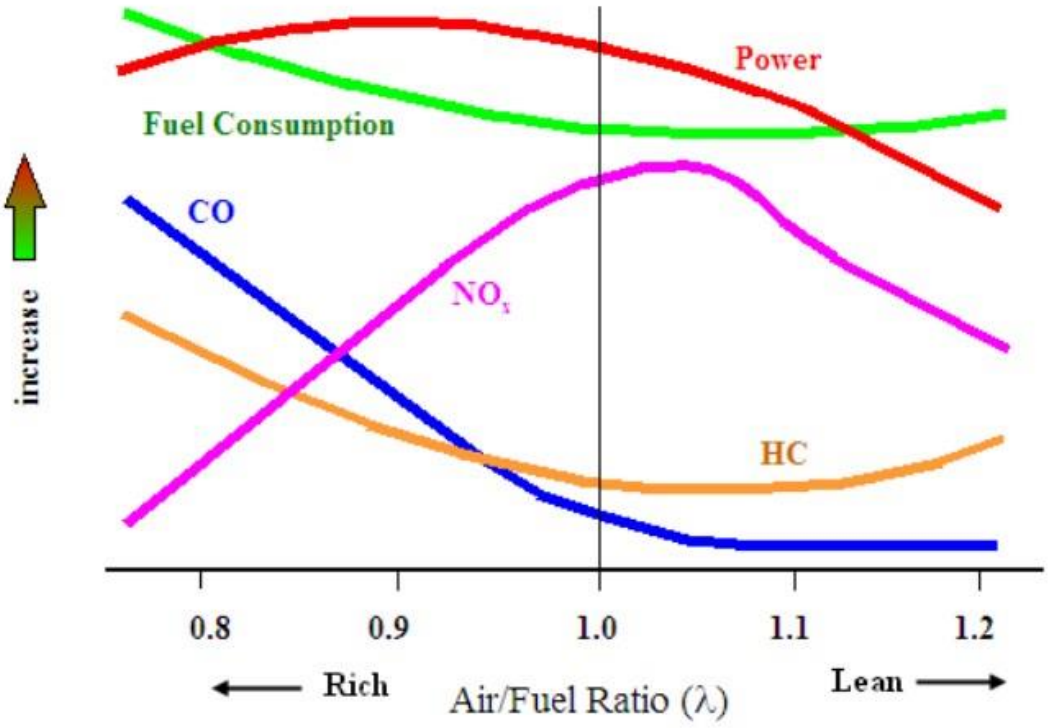

Figure 7: Effect of A/F on combustion

Source: A Comparative Study of a used 4-Stroke Motorcycle Engine Performance [20]

Many researchers have analysed the effect of air to fuel ratio (A/F) on combustion. Most of the previous research were conducted to analyse combustion in internal combustion engines, especially automobile engines because vehicles are responsible to a very high amount of air pollution.

[21] presents the variation of properties of a biogas flame with addition of hydrogen and change of A/F. However, NO_x formation is not analysed in this study.

Figure 7 [20] shows different effects of A/F in a motorcycle engine which use gasoline. Highest power is achieved at rich combustion (x <1) which has higher emissions. Increasing A/F reduce emissions as well as power. Therefore, optimum A/F should be maintained to achieve an economical power with minimum A/F.

Previous researchers have analysed performance of biogas flame combustion and NO_x emissions separately. In this study, variation of performance of biogas flame combustion and NO_x emissions are compared, and range of optimum equivalent ratio for a small-scale combustion chamber is provided. There are several studies on atmospheric dispersion of emissions from combustion for other countries [22], [23]. As a case study, dispersion of emissions from an industrial burner in Colombo area of Sri Lanka is analysed.

1.11.2. Emission dispersion

Emissions of combustion are released to the environment and get dispersed in the atmosphere. The concentration at the releasing point is very high and may exceed hazardous concentration level. Then it gets dispersed in the atmosphere and get diluted. The area which exceeds the hazardous limit must be analysed before implementing the combustor.

Gaussian plume model is a traditional method of calculating pollutant dissipation profiles in the atmosphere. But it does not consider the exhaust temperature and turbulence generated by exhaust gas flow. Previous studies proved that CFD is more accurate in atmospheric dispersion analysis than Gaussian plume model [24].

2. DEVELOPMENT OF MATHEMATICAL MODEL FOR BIOGAS COMBUSTION

2.1. Biogas Combustion

The most often implementation of combustion is in domestic cookers. Most of the heating requirements in Sri Lankan industries are obtained by furnace oil or biomass combustion. Vehicles are powered by gasoline or diesel combustion.

Combustion can be categorized as premixed and non-premixed (diffusion flame). Required oxygen is mixed with fuel before entering the combustion area in premixed flames. Required oxygen in diffusion flame are taken from co-flow or from the environment. When the premixed oxygen amount is not sufficient to complete the combustion, remaining is taken from the environment or from co-flow. That is called partially premixed flame, which is considered in this study.

Biogas mainly contains methane and carbon dioxide. Carbon dioxide is non-reactive, and methane get oxidized.

$$CH_4 + 2O_2 \rightarrow CO_2 + 2H_2O \tag{2.1}$$

One mole of methane needs two moles of oxygen. This mixture is the stoichiometric mixture. If air is used as the oxidant.

$$CH_4 + \frac{2}{0.21}(0.21O_2 + 0.78N_2) \rightarrow CO_2 + 2H_2O + \frac{2}{0.21} \times 0.78N_2 \tag{2.2}$$

Air to fuel ratio (A/F) in the stoichiometric mixture of methane is 0.95.

$$(A/F)_{stoic} = \frac{moles\ of\ air}{moles\ of\ fuel} = \frac{{}^{2}/_{0.21}}{1} = 9.5 \tag{2.3}$$

The ratio between A/F of a partially premixed flame and $(A/F)_{stoic}$ is called 'equivalent ratio' represented by λ.

$$Equivalent\ ratio\ (\lambda) = \frac{(A/F)}{(A/F)_{stoic}} \tag{2.4}$$

2.1. CFD model development

2.1.1. Control volume

In flame combustion control volume is a volume in the considered domain. The control volume is considered as a lumped system. The distributed system which needs to be analysed is divided into a mesh of control volumes. All the control volumes must be small enough to assume as a lumped system.

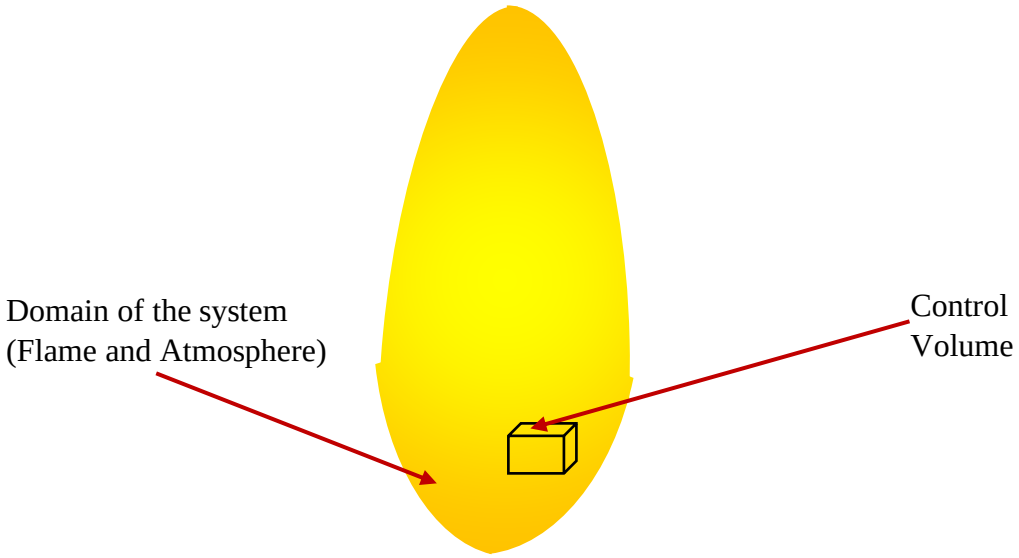

Figure 8: Control volume

2.1.2. Energy transfer inside a control volume

First law of thermodynamics (law of conservation of energy) states that the total energy of an isolated system is constant. Energy can be transformed from one to another but cannot be created or destroyed. For a control volume which is an open system, this can be expresses as (2.5),

$$\dot{Q} - \dot{W} = \sum \dot{m}_e \left(h_e + \frac{v_e^2}{2} + g z_e \right) - \sum \dot{m}_i \left(h_i + \frac{v_i^2}{2} + g z_i \right) \qquad (2.5)$$

2.1.3. Governing equations

There are many CFD models such as finite volume method, finite element method and finite difference method. Finite volume method is used in this research which is simple and easily implementable.

General transport equation for a control volume:

$$\frac{\partial \rho \emptyset}{\partial t} + div(\rho \emptyset v) = div(D\ grad \emptyset) + S_{\emptyset} \tag{2.6}$$

$\emptyset$ is a conservative form of all fluid flow

div($\rho\emptyset$v) is the net rate of flow of $\emptyset$ out of fluid volume (convective term)

$\frac{\partial \rho \emptyset}{\partial t}$ is the net change of $\emptyset$ in the fluid volume

$div(D\ grad \emptyset)$ is the rate of change of $\emptyset$ due to diffusion

$S_{\emptyset}$ is a rate of increase of $\emptyset$ due to source

Only the steady state systems are considered in this study. At steady state:

$$\frac{\partial \rho \emptyset}{\partial t} = 0 \tag{2.7}$$

$$div(\rho \emptyset v) - div(D\ grad \emptyset) - S_{\emptyset} = 0 \tag{2.8}$$

2.1.4. Combustion Model

Combustion is an exothermic redox chemical reaction between a fuel (the reductant) and an oxidant, usually oxygen. The reaction generates heat as well as light in the form of a flame.

The i[th] specie mass fraction transport for a control volume is defined as (2.9).

$$\frac{\partial}{\partial t}(\rho Y_i) + \frac{\partial}{\partial x_j}\left(\rho u_j Y_i\right) = \frac{\partial}{\partial x_j}\left(\rho D_i \frac{\partial Y_i}{\partial x_i}\right) + R_i \tag{2.9}$$

$$R_i = M_{w,i} \sum_{r=1}^{N_R} \hat{R}_{i,r} \tag{2.10}$$

$$\hat{R}_{i,r} = \tau(\nu_{i,r}^{"} - \nu_{i,r}^{'})\left(k_{f,r} \prod_{j=1}^{N_r} [C_{j,r}]^{\eta_{j,r}^{'}} - k_{b,r} \prod_{j=1}^{N_r} [C_{j,r}]^{\eta_{j,r}^{"}} \right) \tag{2.11}$$

$k_{f,r}$ is provided by the Arrhenius equation

$$k_{f,r} = A_r e^{-\frac{E_r}{RT}} \tag{2.12}$$

Energy equation is defined as (2.13)

$$\frac{\partial \rho E}{\partial t} + \nabla.(\rho U E) + \nabla.(Up) = -\nabla.q + \nabla.(\tau.U) + \rho r + \rho g U \tag{2.13}$$

2.1.5. Chemical kinetics

Reaction mechanism of combustion

Combustion process has many parallel and serial reactions. The reaction mechanism with all those reactions is needed for the simulation but solving all those reactions consumes a lot of computation time. Therefore, the reaction mechanism is reduced by removing the reactions with negligible rates. GRIMech [25] is such a published chemical kinetic mechanism. Researchers have proved that GRIMech is valid for biogas combustion simulations. It contains reactions of all three thermal, prompt and fuel NO_x mechanism. H_2S combustion reactions were appended because they are not included in GRIMech [26].

TDAC algorithm

GRIMech has 500 reactions with 60 species which are too much for simulations. Therefore, the mechanism was further reduced real-time during simulation using Tabulation of dynamic adaptive chemistry (TDAC) [27] algorithm.

TDAC is a method which neglects reactions with negligible conversion [28]. Also, it tabulates calculated integration results of each iteration. Then when the same integration was needed to be calculated in future iterations it recalls the tabulated results. This method is called in situ adaptive tabulation (ISAT). Therefore, TDAC solver runs faster than other solvers. Observations showed that TDAC algorithm can speedup a simulation by approximately 2.5 times.

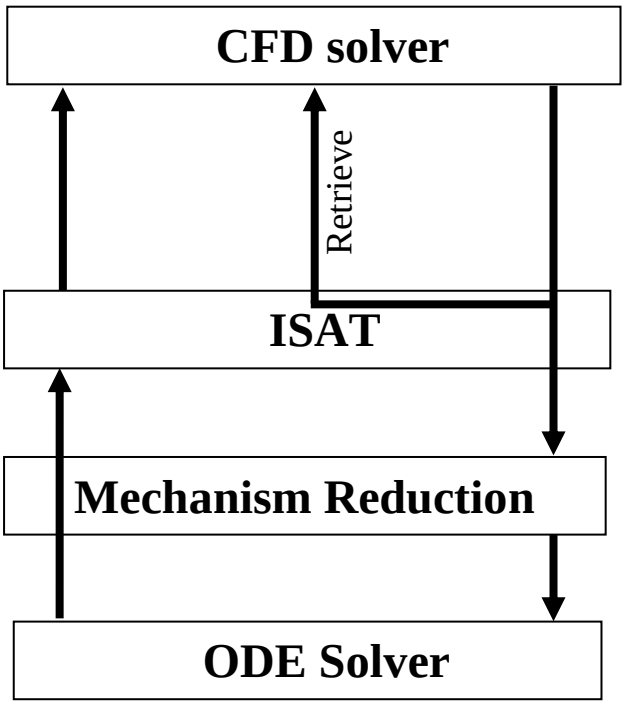

Figure 9: TDAC algorithm

3. CFD SIMULATION FOR DLR FLAME

The developed solver and reaction mechanism used must be validated before using for analysis of combustion systems with it. The accepted method of validation is comparing the simulated results with experimental data. The proposed combustion model was used to simulate and compare a $CH_4/H_2/N_2$ flame with the DLR-Stuttgart $CH_4/H_2/N_2$ Jet Flame A. Details of DLR jet flame are given below.

Fuel (mass percentages): 22.1% CH_4, 33.2% H_2, 44.7% N_2

Fuel inlet velocity: 42.2 m/s

Inlet Re: 15200

Fuel Nozzle diameter: 8mm

Co-flow velocity: 0.3m/s

Co flow diameter: 360mm

Co flow temperature: 292K

Inlet temperature: 292K

3.1. Development of CFD model for DLR flame

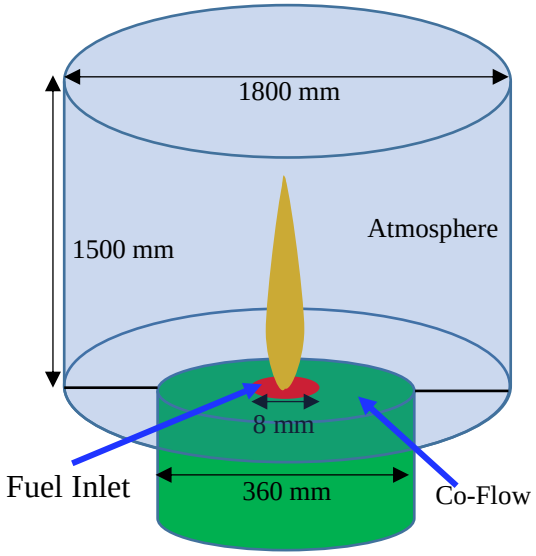

Figure 10: Geometry of simulation mesh

Required minimum length and diameter of simulated atmosphere was observed as 1.5m and 1.8m to get the best accuracy.

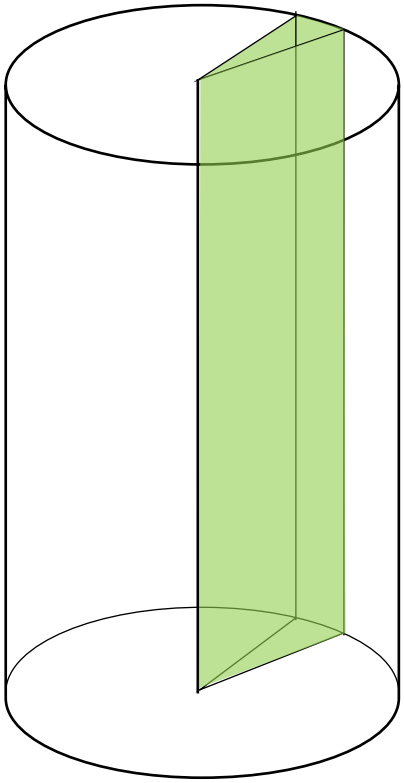

Figure 11: 2D Wedge

The combustor is a cylinder. Simulating a 3D cylinder consumes a lot of computation power. A 2D wedge was selected as the domain of simulation as the system is axisymmetric. Required processing time is very low for 2D simulation compared to 3D simulation.

Assumptions on wedge plane

- The fluxes across a wedge plane are zero
- The normal components of all variables are set to zero

Different mesh sizes were simulated to finalize the suitable mesh size in the study and selected 40×50 cells for the domain as in Figure 12. Observed that the number of cells in the co-flow area below the flame has a negligible effect.

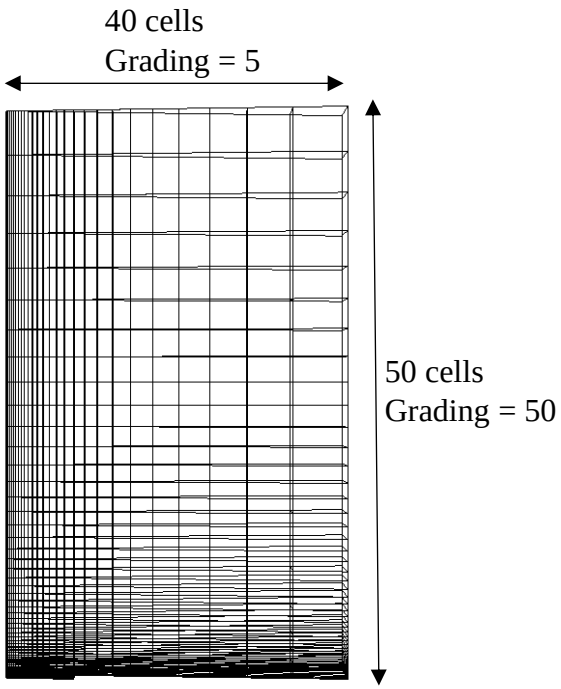

Figure 12: 2D wedge mesh which is used for simulation

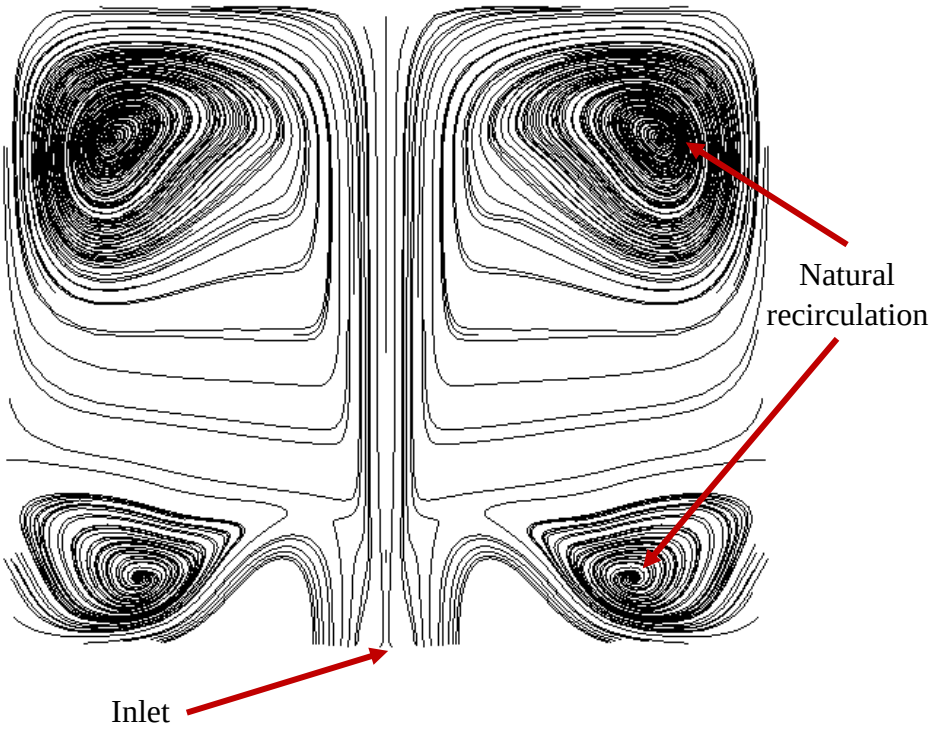

Figure 13: Flow pattern

There is a natural recirculation in the atmosphere. Sufficient volume of the atmosphere must be included in the simulation as shown in Figure 10 to simulate the effect of recirculation accurately.

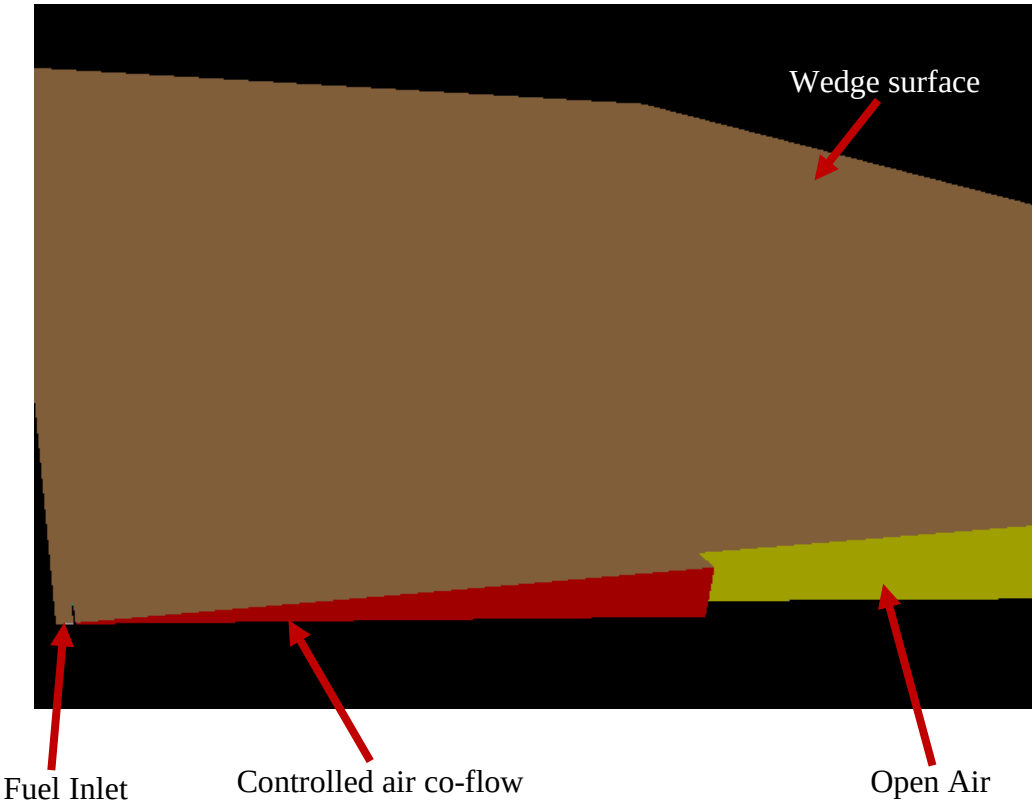

Figure 14: Inlets

Table 4: Boundary conditions of DLR flame simulation

Property	**Boundary**	**OpenFOAM boundary type /Value**	**Remarks**
Temperature	Fuel Inlet	fixedValue (298K)	Room temperature
	Air co-flow	fixedValue (298K)	Room temperature
	Open air	zeroGradient	Zero Gradient - Heat conduction to the environment is negligible relative to convection
	Wedge surface	wedge	2D simulation
Velocity	Fuel Inlet	fixedValue (42.2m/s)	Experimental value
	Air co-flow	fixedValue (0.3m/s)	Experimental value

	Open air	pressureInletOutletVelocity;	Velocity is calculated based on pressure difference
	Wedge surface	wedge	2D simulation
Pressure	Fuel Inlet	zeroGradient	Zero Gradient
	Air co-flow	zeroGradient	Zero Gradient
	Open air	totalPressure (1 atm)	Open to the environment
	Wedge surface	wedge	2D simulation
Specie	Fuel Inlet	fixedValue (22.1% CH_4, 33.2% H_2, 44.7% N_2)	Experimental value (Mass percentage)
	Air co-flow	fixedValue (23% N_2, 77% O_2)	Air supply
	Open air	zeroGradient	zeroGradient – No mass transfer from environment to the exhaust
	Wedge surface	wedge	2D simulation

There are mainly three turbulence models used in CFD as Direct Numerical Simulation (DNS) [29], large eddy simulation (LES) [30] and Reynolds Averaged Navier-Stokes (RANS) [31]. DNS is the most accurate model and it consumes the highest computation time. LES is faster than DNS and more accurate than RANS. RANS is the fastest. Even though RANS is the least accurate compared to the other two turbulent models, RANS gives sufficient accuracy in DLR flame simulation. Therefore, RANS was selected as the turbulent model in DLR flame simulation considering accuracy and available computation power.

There are mainly two RANS models as k-ε and k-ω [32]. k-ω model is recommended when wall effect is very high and k- ε model is recommended when the fluid flow far away of the wall is significant. The turbulent model used in DLR flame simulation is k- ε because the flame is far away from walls. Estimated best k- ε parameters for the simulation are presented in Table 5.

Table 5: Turbulent parameters

	k – Turbulent Intensity	ε – Mixing Length
Fuel Inlet	0.03	0.005
Air Inlet	0.02	0.005

3.2. Model Validation

Following experimental data of axial and radial profiles of DLR flame are published by previous researchers [7].

Axial profiles

- Temperature
- Velocity
- Species (O_2, H_2, CH_4, H_2O, CO_2, CO)

Locations of axial data points are presented in Figure 15-Figure 18

Radial profiles

- Velocity (at 0.1, 4, 8, 16, 32, 48 cm axial distances)

Locations of radial data points of each profile are presented in Figure 22-Figure 28

Simulation data of developed model were compared with those experimental data in order to analyse the accuracy of the developed model.

3.2.1. Axial profile comparison of DLR flame

Axial temperature, velocity and specie profiles of simulation were compared with experimental results.

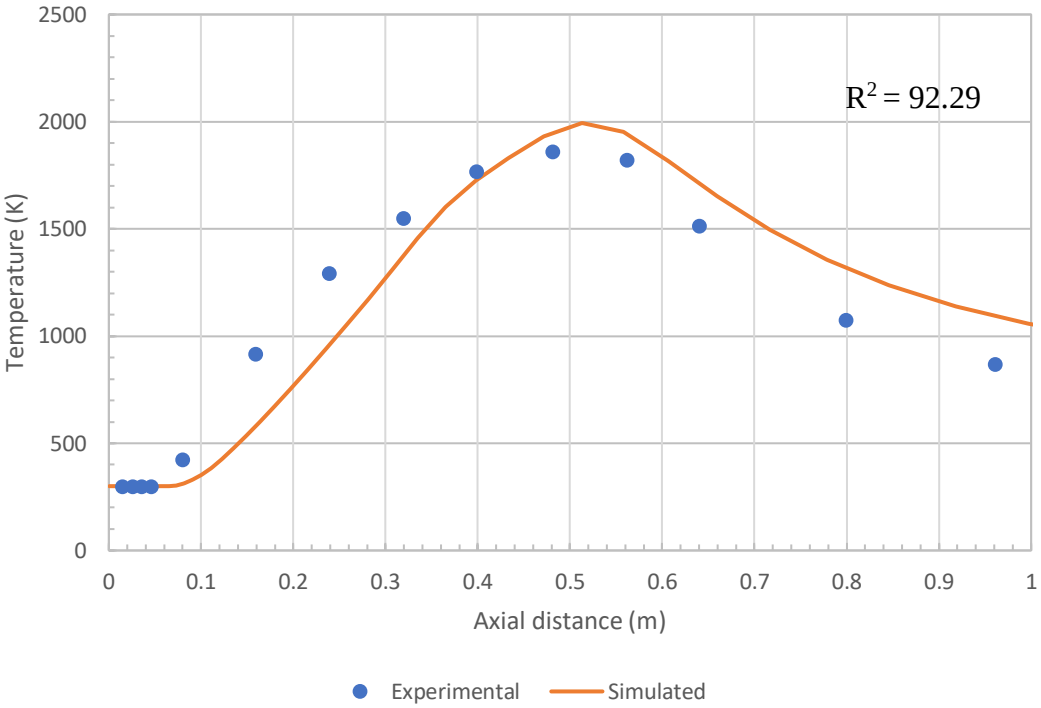

Figure 15: Axial Temperature profile of DLR flame

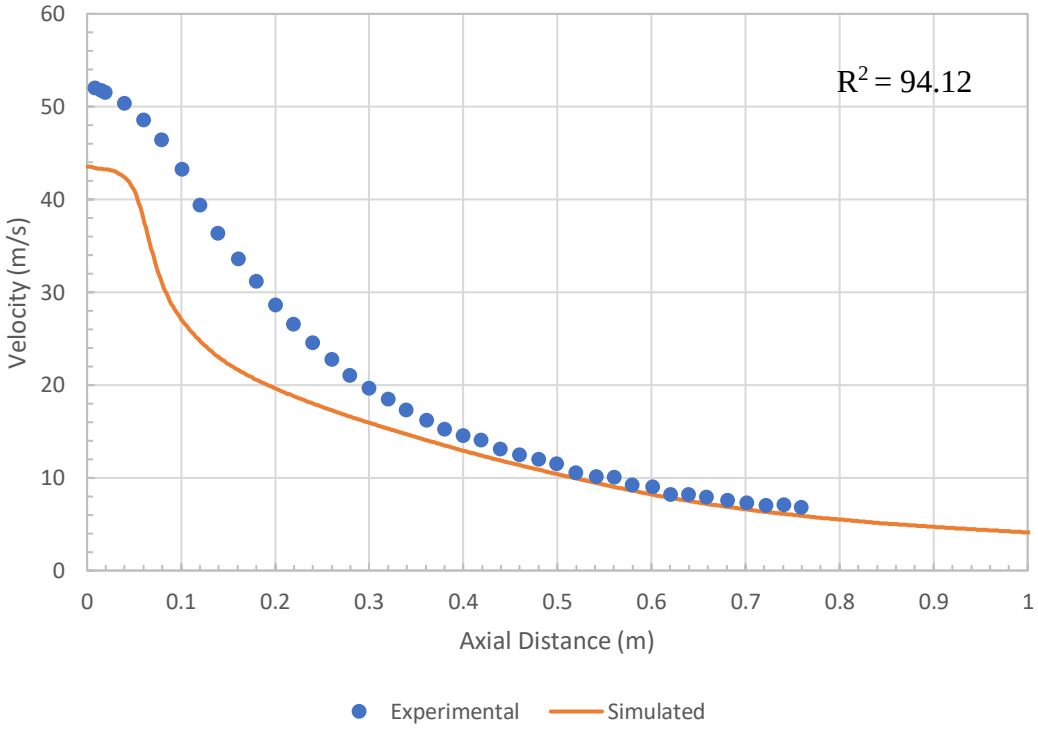

Figure 16: Axial Velocity Profile of DLR Flame

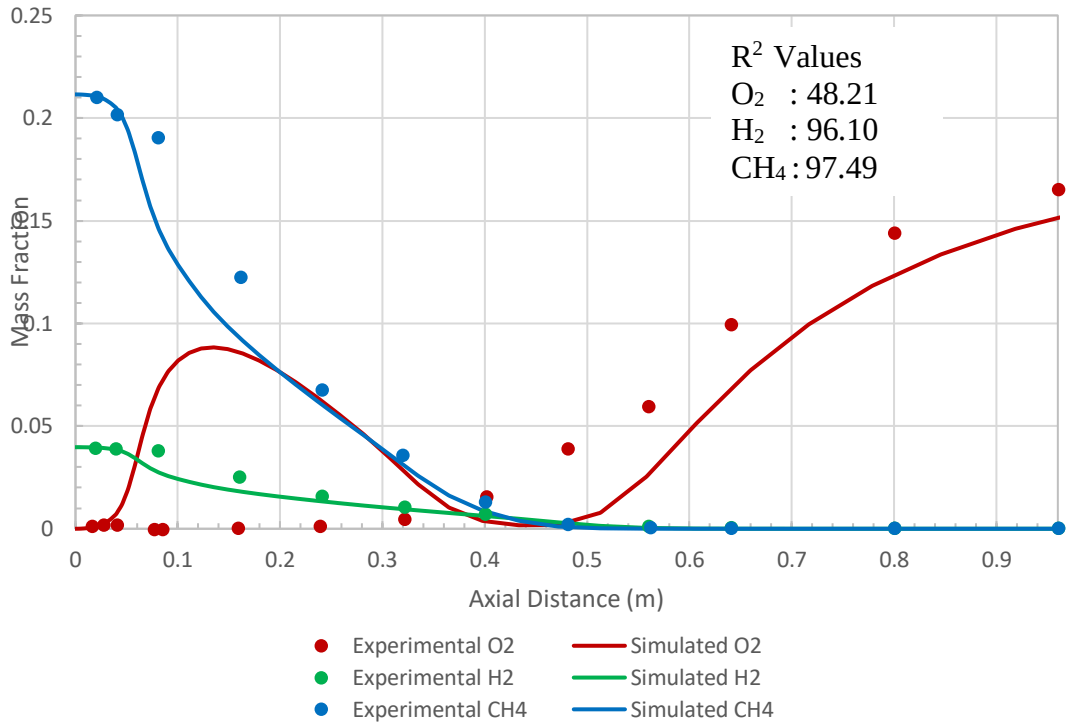

Figure 17: Axial Specie Concentrations of DLR Flame

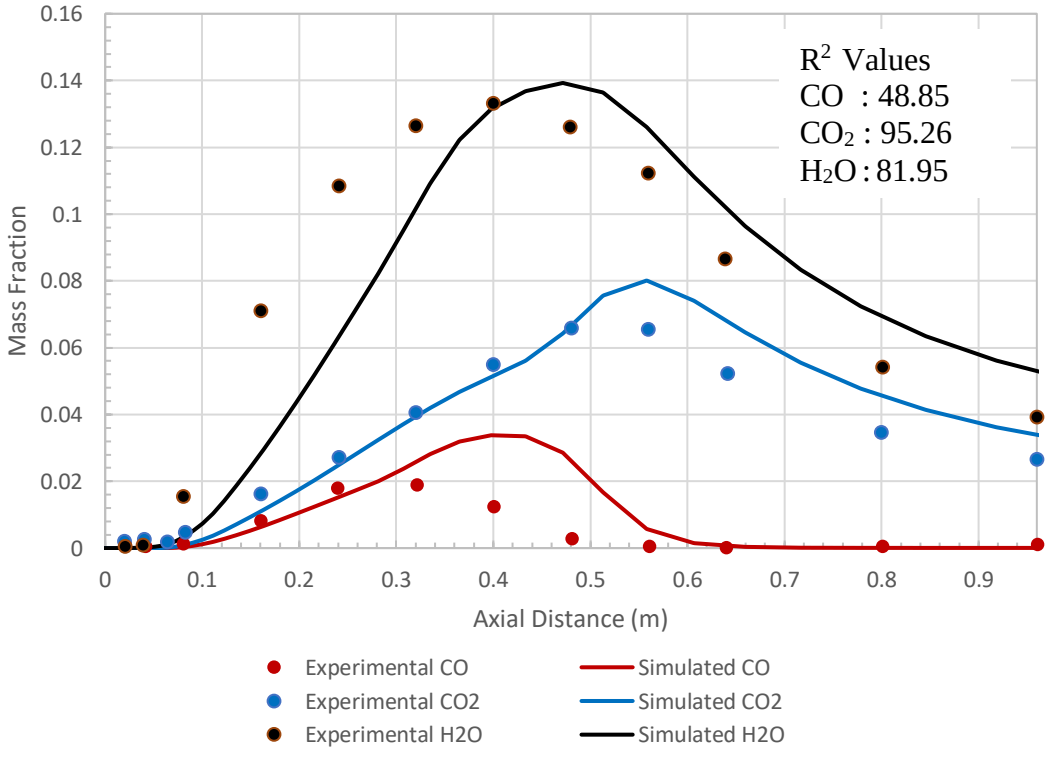

Figure 18: Axial Specie Concentrations of DLR Flame

Simulation results were compared with published simulation results of J.-Y. Chen (UC Berkeley) [7].

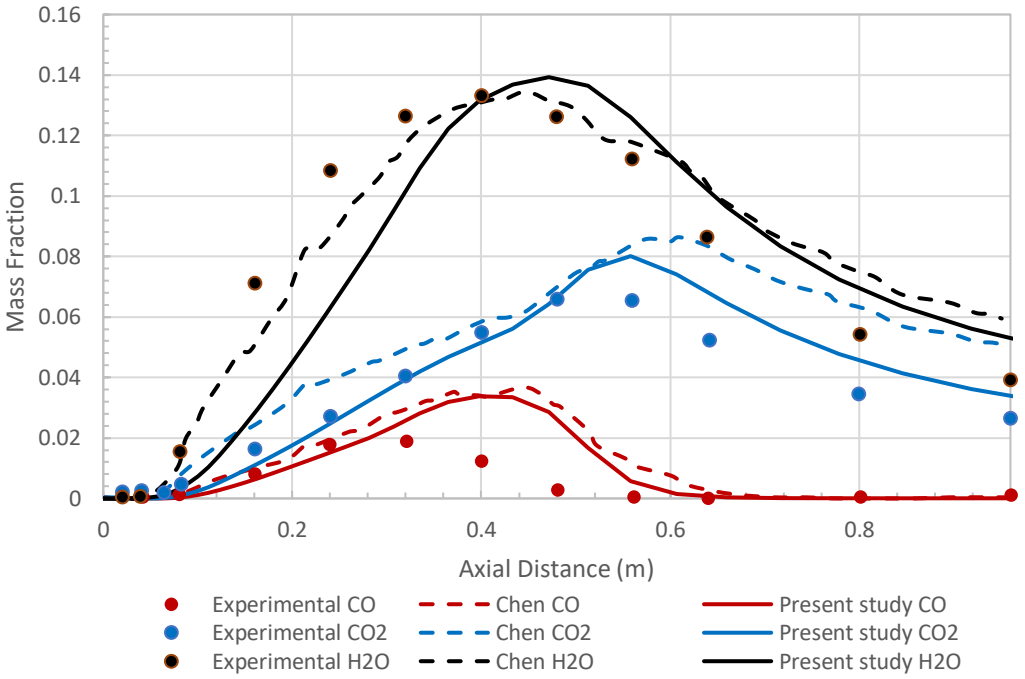

Figure 19: Comparison with published simulation results of DLR Flame

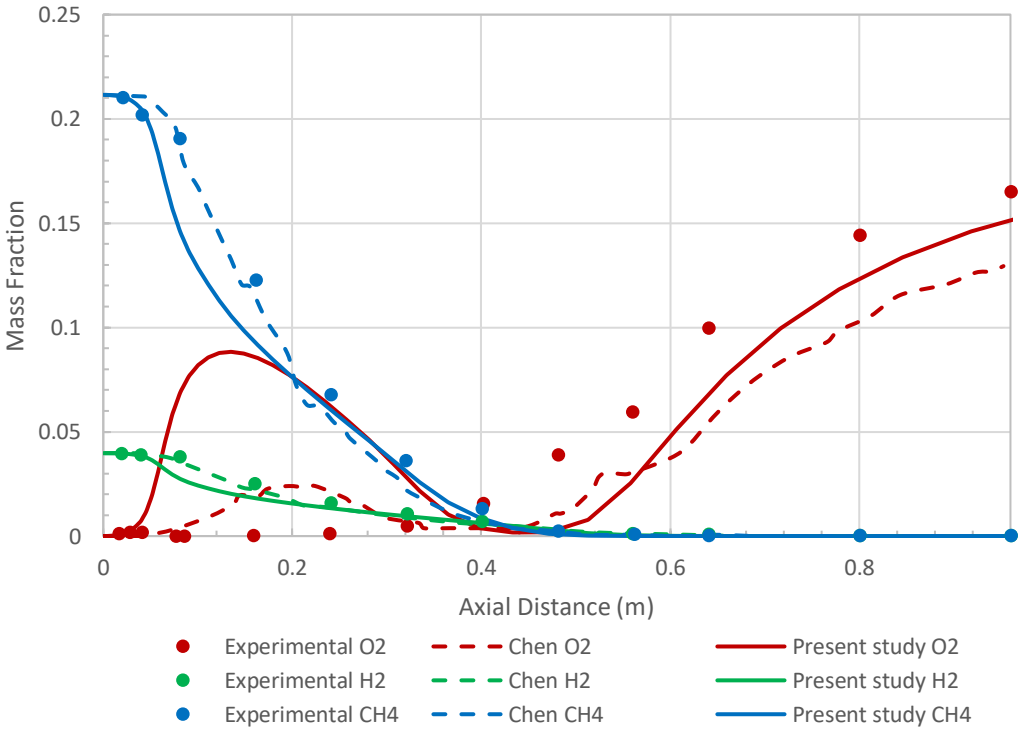

Figure 20: Comparison with published simulation results of DLR Flame

Results of present study tally more with simulation results of J.-Y. Chen (UC Berkeley) than experimental data. However, results of J.-Y. Chen are more accurate

because it uses a reaction mechanism which is customized for DLR flame. GRIMech which is used in this study is a general reaction mechanism which is suitable for any combustion system which uses hydrocarbons with less than 3 carbon atoms and hydrogen as the fuel. The fuel used in this study is biogas which is a mixture of methane and carbon dioxide. Therefore, GRIMech is used in this study.

3.2.2. Radial profile comparison of DLR flame

Experimental radial velocity profiles shown in Figure 21 were compared with simulation results.

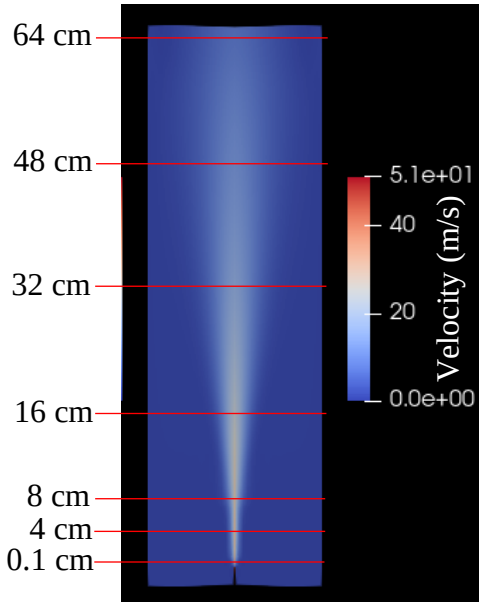

Figure 21: Axial distances to the radial profiles considered in validation

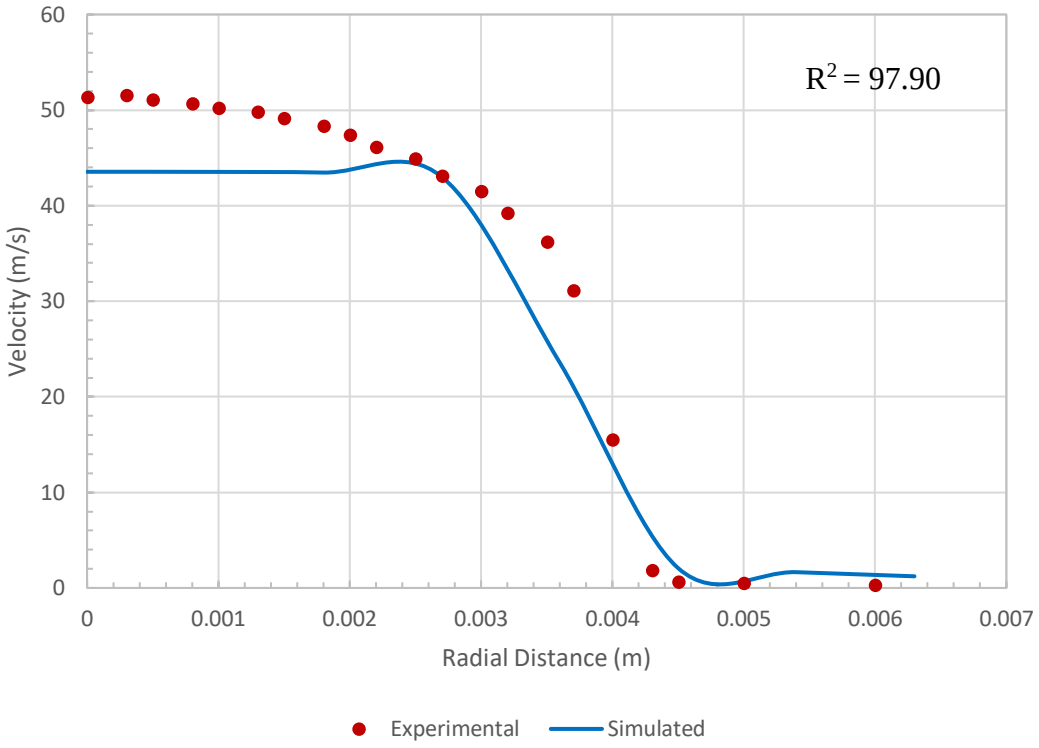

Figure 22: Radial velocity profile at 0.001m axial distance

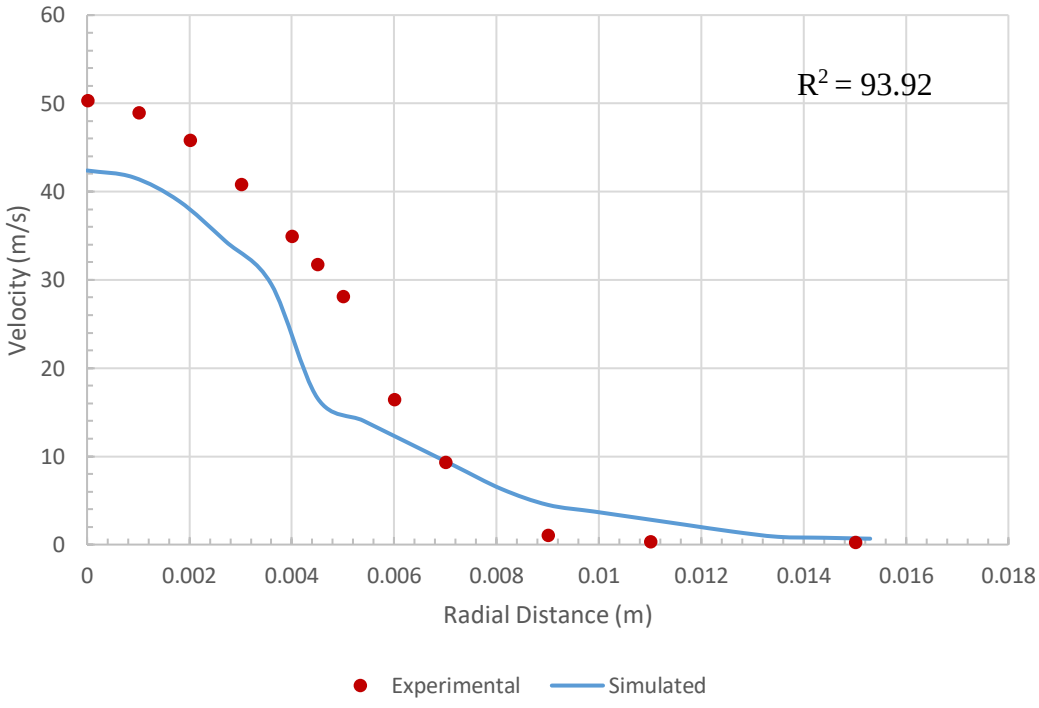

Figure 23: Radial velocity profile at 0.04m axial distance

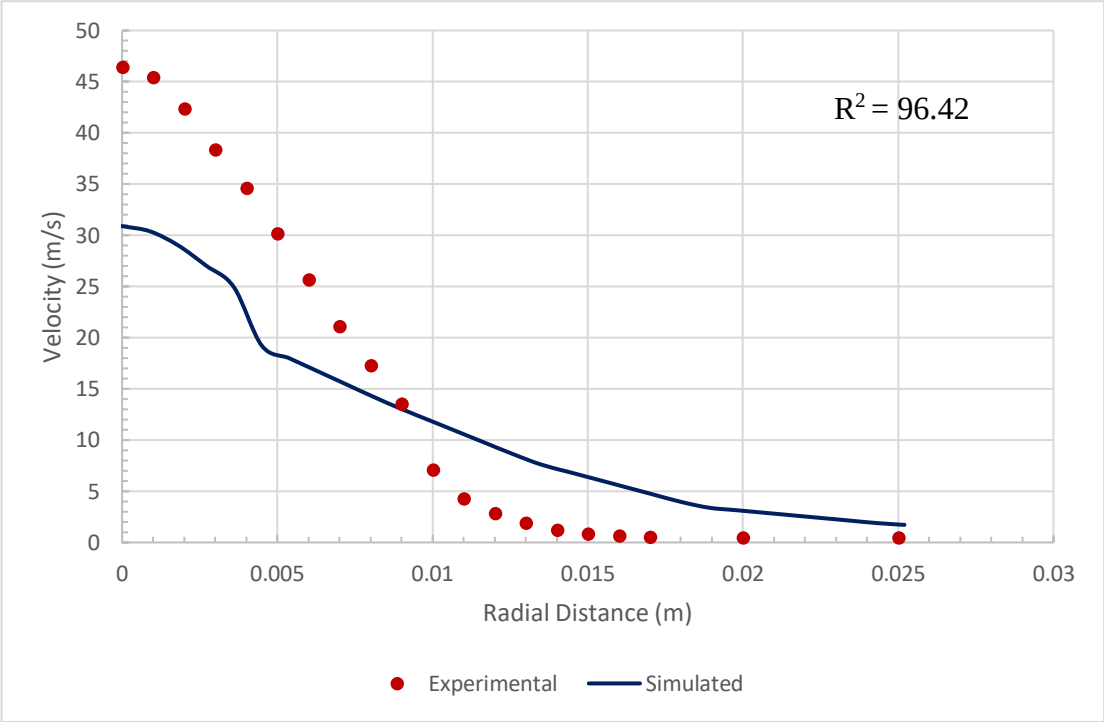

Figure 24: Radial velocity profile at 0.08m axial distance

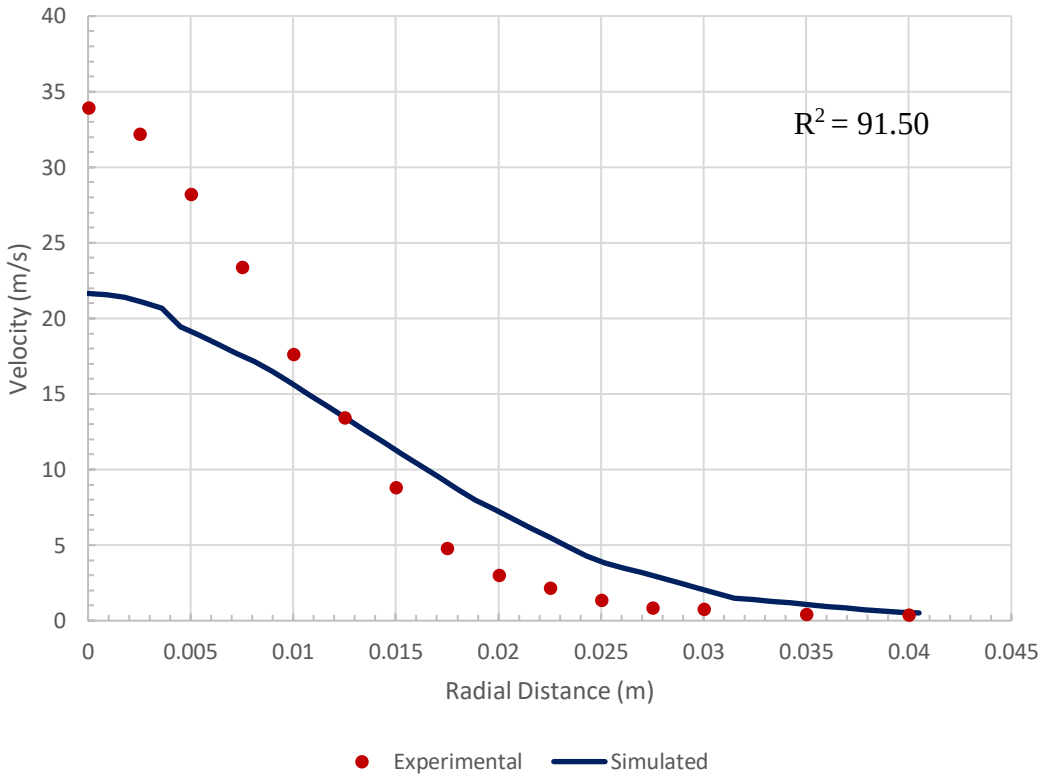

Figure 25: Radial velocity profile at 0.16m axial distance

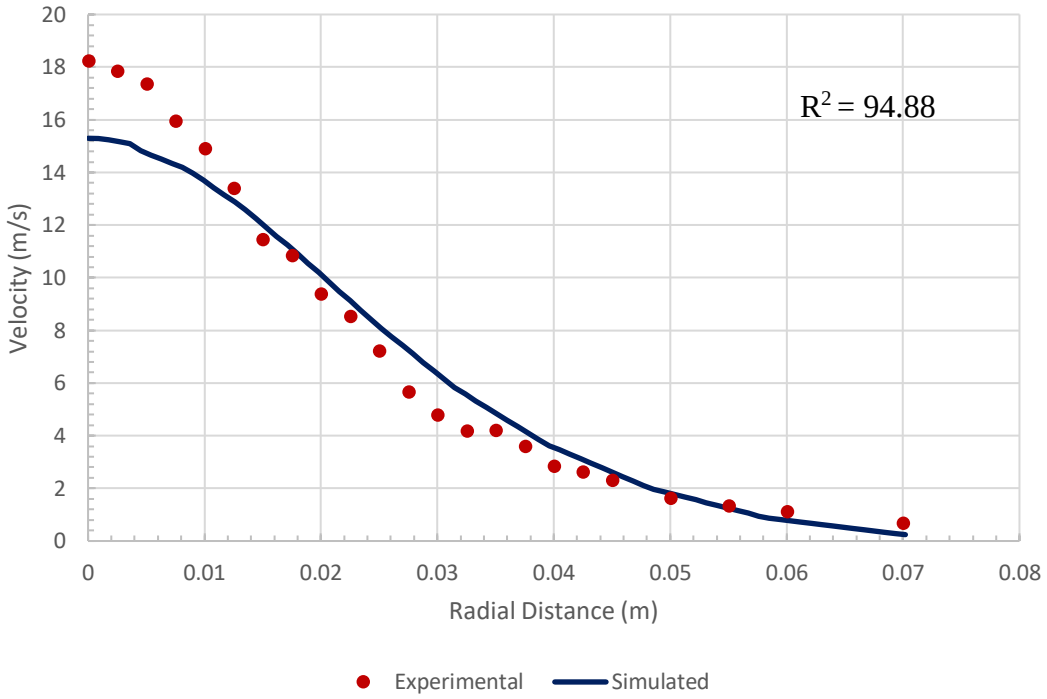

Figure 26: Radial velocity profile at 0.32m axial distance

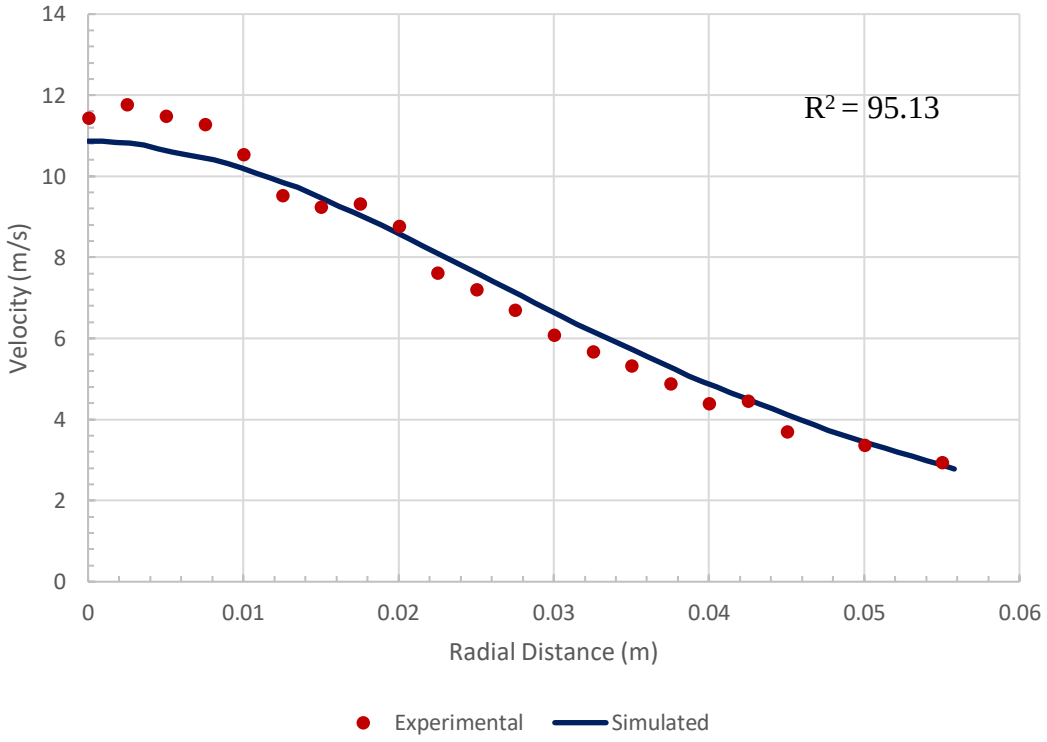

Figure 27: Radial velocity profile at 0.48m axial distance

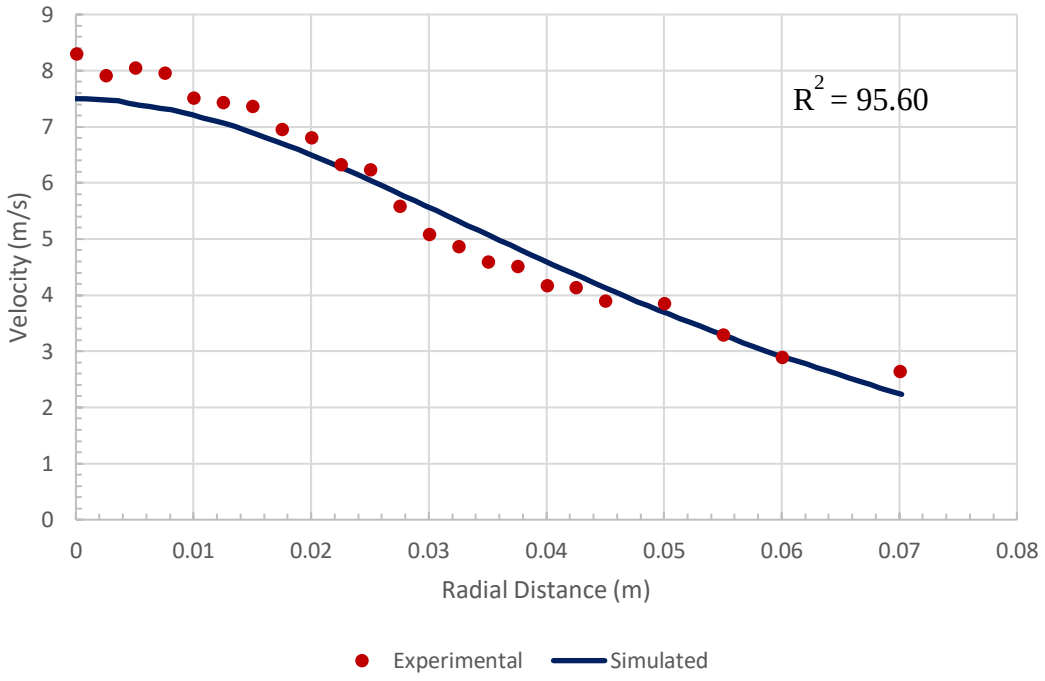

Figure 28: Radial velocity profile at 0.64m axial distance

To evaluate the accuracy of the model, R-Squared value comparing simulated and experimental data were calculated.

R Squared value (Coefficient of Determination) can be defined as:

$$R^2 = \frac{n(\sum xy) - (\sum x)(\sum y)}{\sqrt{\left[n\sum x^2 - (\sum x)^2\right]\left[n\sum y^2 - (\sum y)^2\right]}} \quad (3.1)$$

Where, 'x' is actual value, 'y' is predicted value and 'n' is number of values

R-Squared values of experimental and simulated radial velocity profiles are presented in Table 6. All of the values are above 90%.

Table 6: R-Squared values of radial velocity comparison

Axial Distance (cm)	**R-Squared value – R^2 (%)**
0.1	97.90
4	93.92
8	96.42
16	91.50
32	94.88
48	95.13
64	95.60

R-Squired values of axial profiles are presented in Table 7.

Table 7: R-Squared values of axial profile comparison

Profile	**R-Squared value – R^2 (%)**
Temperature	92.29
Velocity	94.12
O_2	48.21
H_2	96.10
CH_4	97.49
CO	48.85
CO_2	95.26
H_2O	81.95

R-Squared value of axial profile comparison are above 80% except for O_2 and CO. H. Pitsch (UC San Diego) has published more accurate simulation results [7] as LES turbulence model is used. Present study uses a RANS model in order to reduce the required computation time.

4. MODELLING OF SMALL-SCALE BIOGAS COMBUSTION CHAMBER

Biogas composition depends on the type of biomass source, the type of microorganisms available and the amount of air available. Therefore, biogas composition varies with time. Average compositions of biogas were used for the simulation [33], [34], [35], which are shown in Table 8.

Table 8: Biogas Composition

Component	Mass fraction
CH_4	4.997×10^{-1}
CO_2	4.072×10^{-1}
H_2O	4.820×10^{-2}
N_2	1.249×10^{-2}
O_2	2.856×10^{-2}
H_2S	3.792×10^{-3}
NH_3	5.689×10^{-5}

Source: [33], [34], [35]

The emissions of biogas combustion were analysed considering a small-scale experimental setup.

4.1. Mesh generation of small-scale combustion chamber

Biogas can be burnt as a flare or in a chamber as in Figure 29, which permits better control to reduce emissions, which is considered in this study. Air co-flow of the

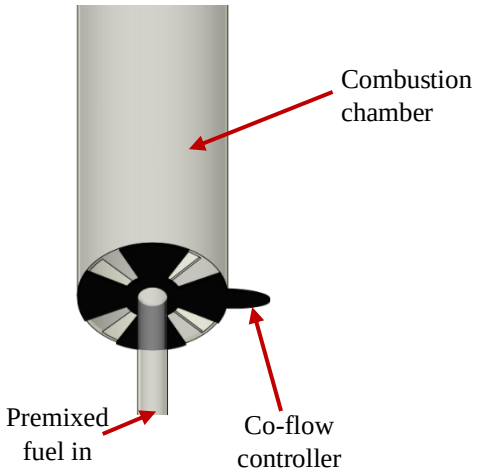

Figure 29: Small-scale experimental setup

considered combustion chamber can be controlled. In this study assumed that the co-flow is fully open.

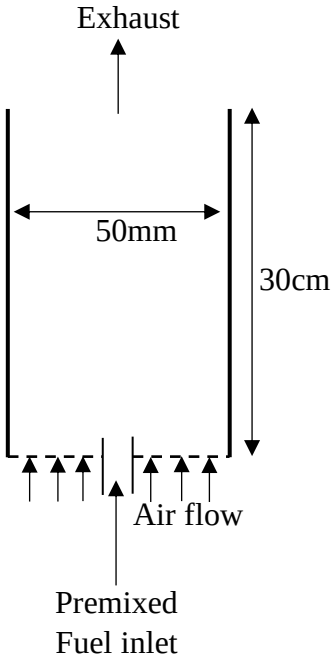

Figure 30: Dimensions of small-scale Combustion chamber

Table 9: Parameters of Combustion Chamber Simulation

Parameter	**Value**
Premixed fuel flow rate	0.1m/s
Air co-flow	Natural draft
Wall	2mm thick stainless steel
Wall outside environment	100 °C boiling water
Chamber diameter	50mm
Nozzle diameter	5mm
Simulated chamber height	0.3m

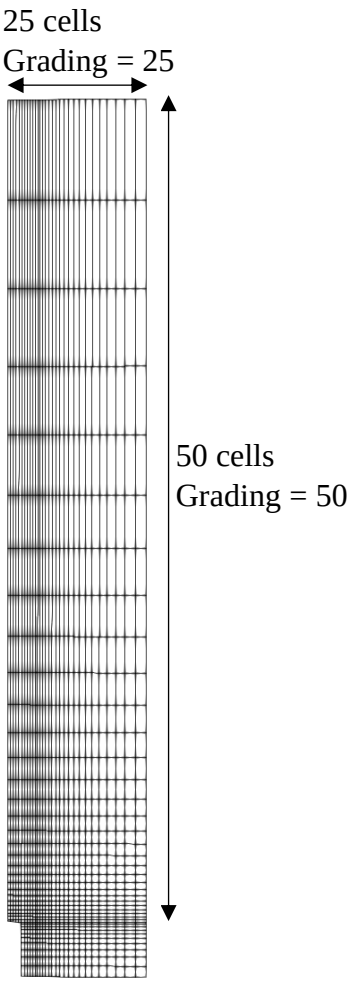

Figure 31: Mesh size of small-scale combustion chamber

Different mesh sizes were simulated to finalize the suitable mesh size in the study and selected 25×50 cells for the domain as in Figure 31. Observed that the number of cells in the co-flow area below the flame has a negligible effect.

4.2. CFD model

The same CFD model used to simulate the DLR flame was used to simulate the small-scale combustion chamber.

4.2.1. Solver development

There are many solvers in OpenFOAM which can be used combustion simulations. They are explained below:

chemFoam: This can simulate reactions at a point

reactingFoam: This can simulate reactions in a 2D or 3D profile. Gravity is neglected

buoyantReactingFoam: This can simulate reactions in a 2D or 3D profile with considering Gravity

chtMultiRegionFoam: This can simulate reactions in a 2D or 3D profile which consist of many regions of fluid and solid. Gravity is considered. Wall heat loss can be accurately simulated.

Best solver for the considered system is chtMultiRegionFoam. But this solver consumes a lot of processing time. Therefore, buoyantReactingFoam was used. Heat loss through the wall was implemented as a boundary function in the solver source code.

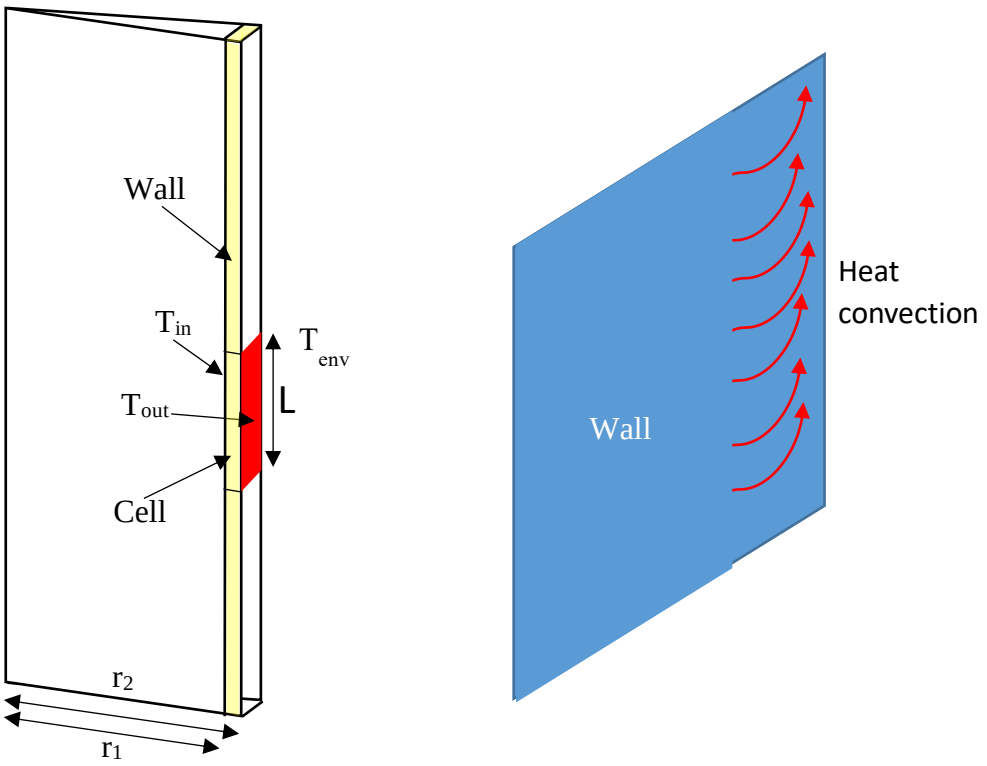

Figure 32: Heat loss from the wall

r_1 -inner radius

r_2 – outer radius

L – axial length of the cell

T_{in} – inner wall temperature

T_{out} - outer wall temperature

T_{env} - environment wall temperature

Conduction heat resistance (Fourier's law)

$$R_1 = \frac{ln\left(\frac{r_2}{r_1}\right)}{2\pi Lk(T_{in}-T_{out})} \times \frac{2\pi r_1}{l}$$

$$= \frac{ln\left(\frac{r_2}{r_1}\right)}{Lk(T_{in}-T_{out})} \times \frac{r_1}{l} \quad (4.1)$$

Convection heat resistance (Newton's cooling law)

$$R_2 = \frac{1}{h \times 2\pi r_2 L(T_{out}-T_{env})} \times \frac{2\pi r_1}{l}$$

$$= \frac{1}{h \times r_2 L(T_{out}-T_{env})} \times \frac{r_1}{l} \quad (4.2)$$

Total heat resistance = $R_1 + R_2$

$$\Delta h = \frac{T_{in}-T_{env}}{R_1+R_2} \times \Delta t \quad (4.3)$$

GRIMech was used to simulate reactions. Assumed H_2S in fuel is completely removed.

Table 10: Boundary conditions of small-scale combustion chamber

Property	**Boundary**	**OpenFOAM boundary type /Value**	**Remarks**
Temperature	Fuel Inlet	fixedValue (298K)	Room temperature
	Air Inlet	fixedValue (298K)	Room temperature
	Outlet	zeroGradient	Zero Gradient - Heat conduction in the exhaust is

			negligible relative to convection
	Wall	Boundary Function as (4.3)	Heat loss as in Figure 33
	Wedge surface	wedge	2D simulation
Velocity	Inlet	fixedValue (0.1m/s)	Inlet velocity of proposed combustion chamber
	Air Inlet	zeroGradient	
	Outlet	pressureInletOutletVelocity;	Velocity is calculated based on pressure
	Wall	noSlip	No mass transfer at the wall
	Wedge surface	wedge	2D simulation
Pressure	Inlet	zeroGradient	Zero Gradient
	Air Inlet	totalPressure (1atm)	Open to the atmosphere
	Outlet	totalPressure (1atm)	Open to the atmosphere
	Wall	zeroGradient	Zero Gradient
	Wedge surface	wedge	2D simulation
Specie	Fuel Inlet	fixedValue (Mass percentages of Biogas/Air mixture)	Composition depends on equivalent ratio
	Air Inlet	fixedValue (23% N_2, 77% O_2)	Open to the atmosphere
	Outlet	zeroGradient	Zero Gradient - No mass transfer from environment to the exhaust
	Wall	zeroGradient	Zero Gradient - No mass transfer at the wall
	Wedge surface	wedge	2D simulation

The flow is laminar if the Reynold number is below 2100 [36]. No turbulent model is implemented as the flow is laminar because of very low Reynold number of 17.

4.3. Equivalent Ratio Analysis

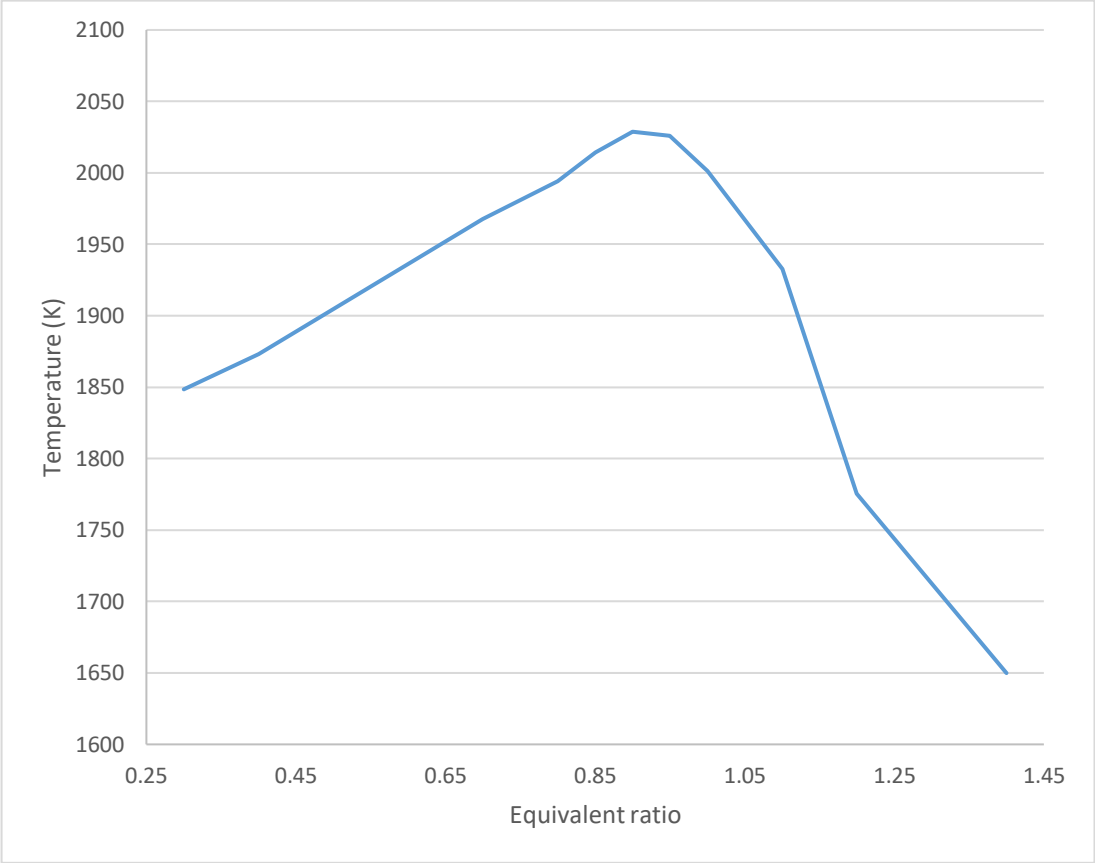

Figure 33: Maximum flame temperature

Maximum flame temperature is at 0.9 equivalent ratio.

To analyse the flame combustion, temperature zones of the simulated flame are presented in Figure 34.

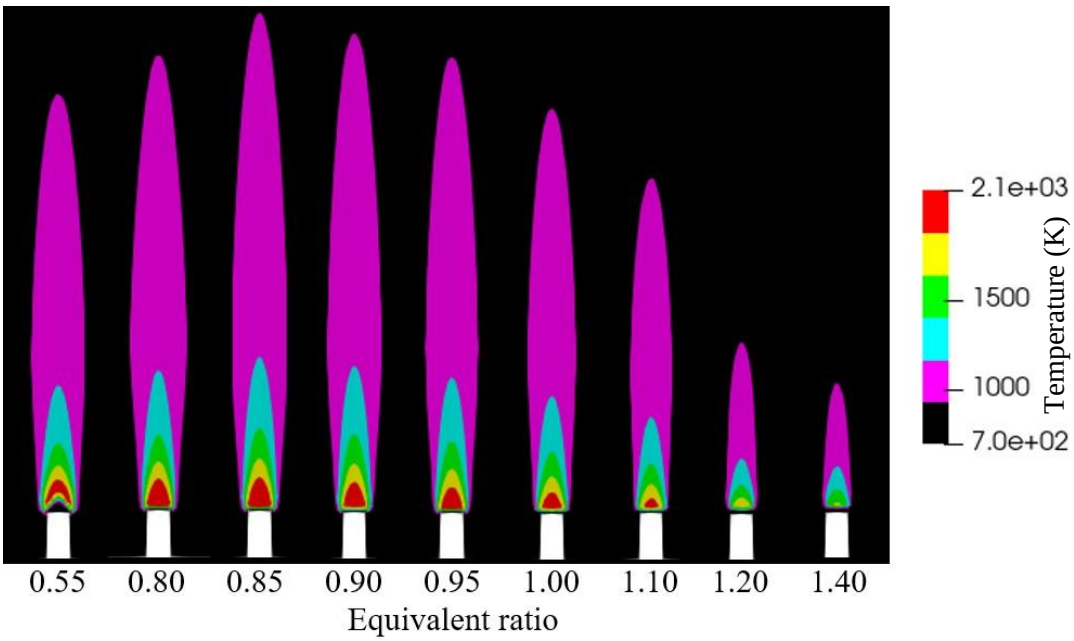

Figure 34: Temperature profile vs equivalent ratio

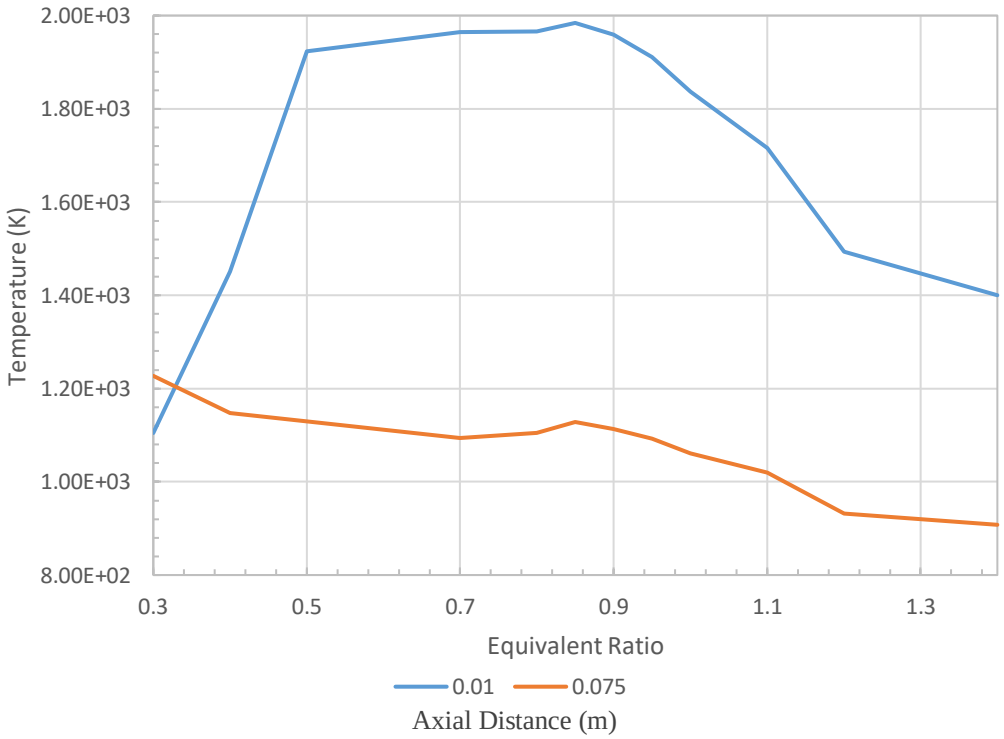

Figure 35: Temperature at different axial distances

Equivalent ratio of 0.85 has the highest temperature at 0.01m axial distance temperature.

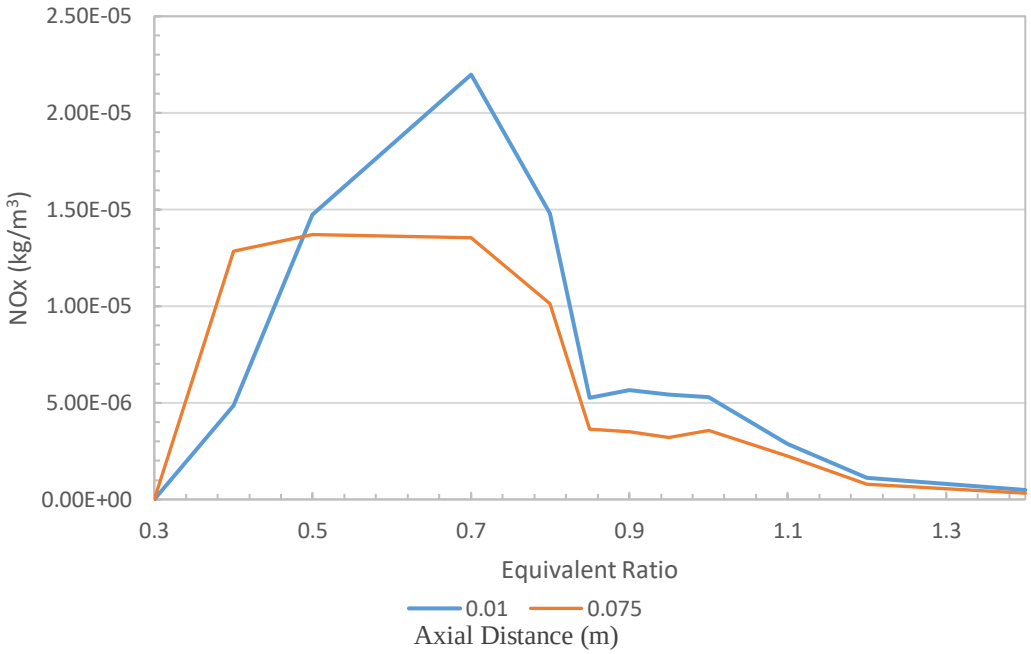

Figure 36: NO_x × rho vs Axial Distance

Equivalent ratio 0.7 has the highest NO_x emission

There is a very high NO_x emission from 0.7 to 0.85 equivalent ratio. It is almost constant from 0.85 - 1 Equivalent ratio.

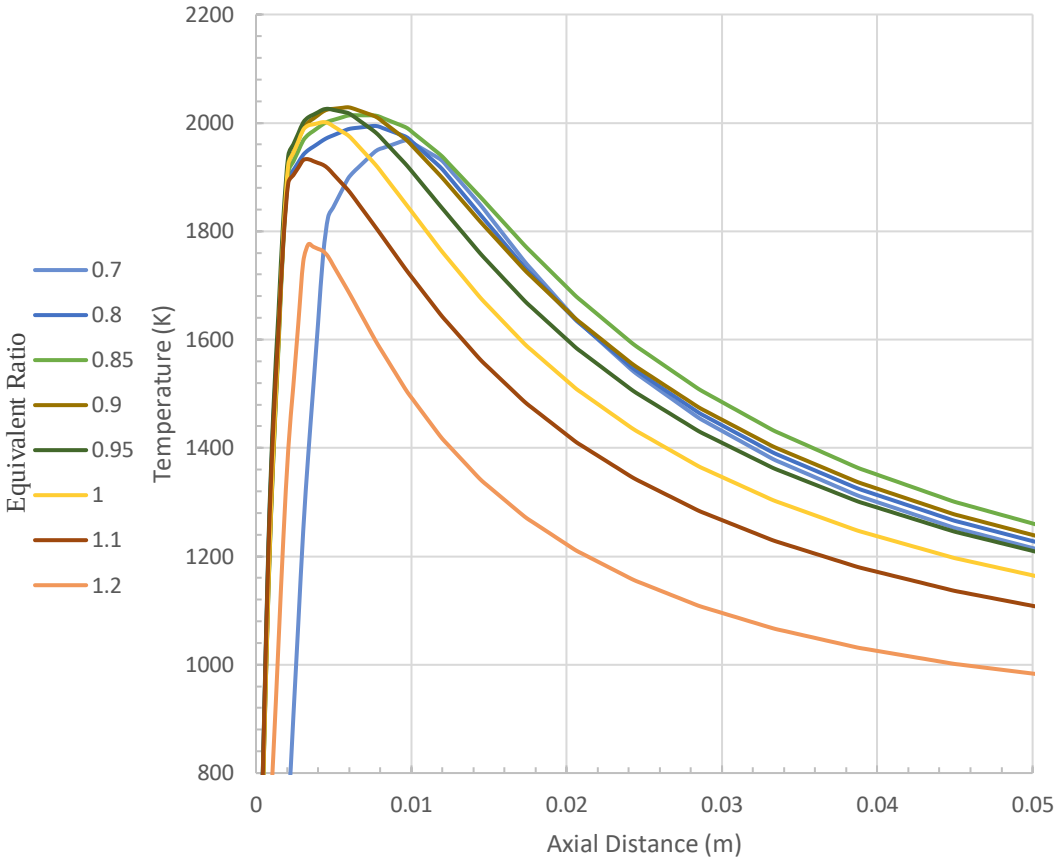

Figure 37: Axial Temperature Profile

According to Figure 33, 0.9 Equivalent ratio has the maximum peak temperature. However, 0.85 equivalent ratio has the overall highest flame temperature as shown in Figure 37. The highest flame length is at 0.85 equivalent ratio as shown in Figure 34.

$$\text{Heat output} = \oiiint Temperature \cdot dv \tag{4.4}$$

Heat output depends on temperature and flame size according to (4.4). Therefore, the maximum heat output is at 0.85 equivalent ratio.

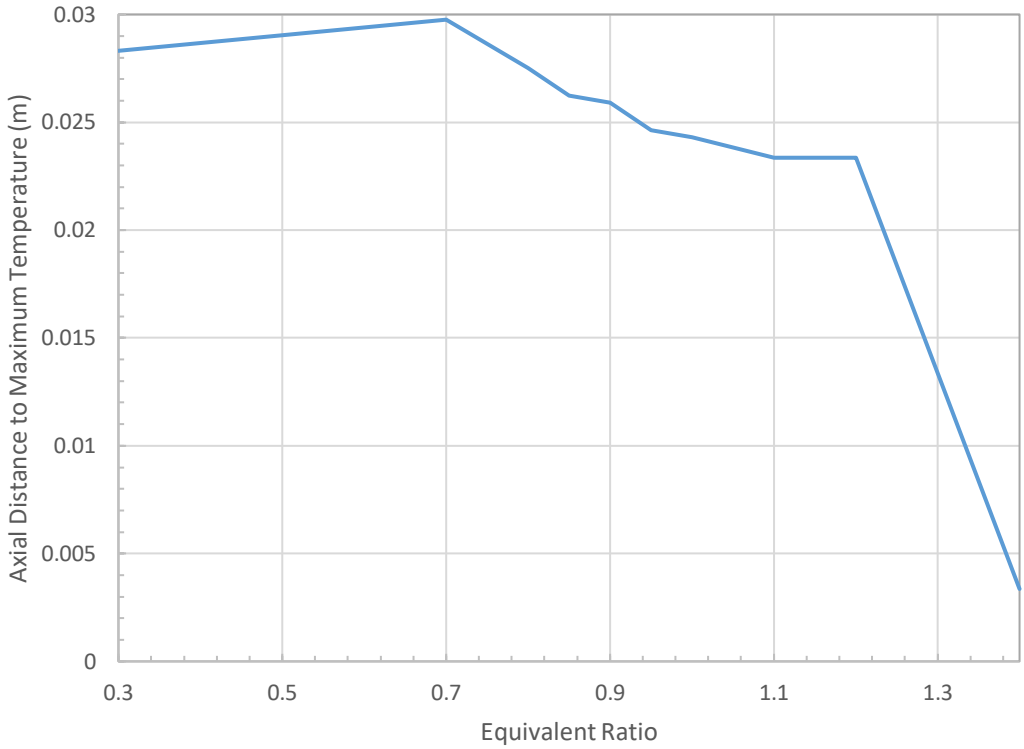

Figure 38: Axial distance to the location with highest temperature

Figure 38 presents the axial distance to the maximum temperature point from the nozzle. The highest distance can be observed at equivalent ratio of 0.7. This distance is very low in equivalent ratios above 1.2

Figure 39 compares O_2, H_2O mass fractions and heat release rate (Q) at the different equivalent ratios (ER). Generally, heat release rate is proportional to the reaction rate.

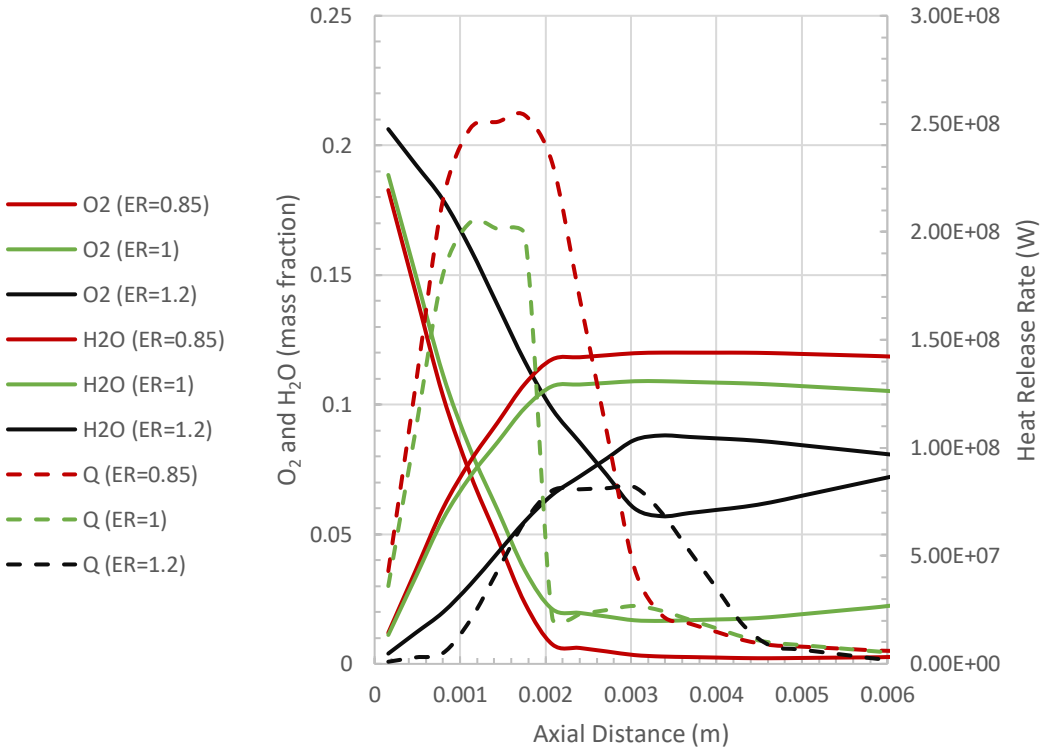

Figure 39: Axial concentrations and heat release rate profile

At the inlet, there is a high concentration of O_2 as the fuel is premixed. Then the concentration drops along the centreline as it is consumed by the reaction. Then it increases again by the diffusion of O_2 from co-flow. At the 0.85 equivalent ratio, O_2 concentration drops up to 0.002m axial distance. However, heat release happens up to 0.003m due to diffused oxygen is present even though premixed oxygen is not sufficient. At the 1.2 equivalent ratio, reaction completes at the axial distance of 0.0035m before O_2 concentration drops as there is sufficient premixed O_2.

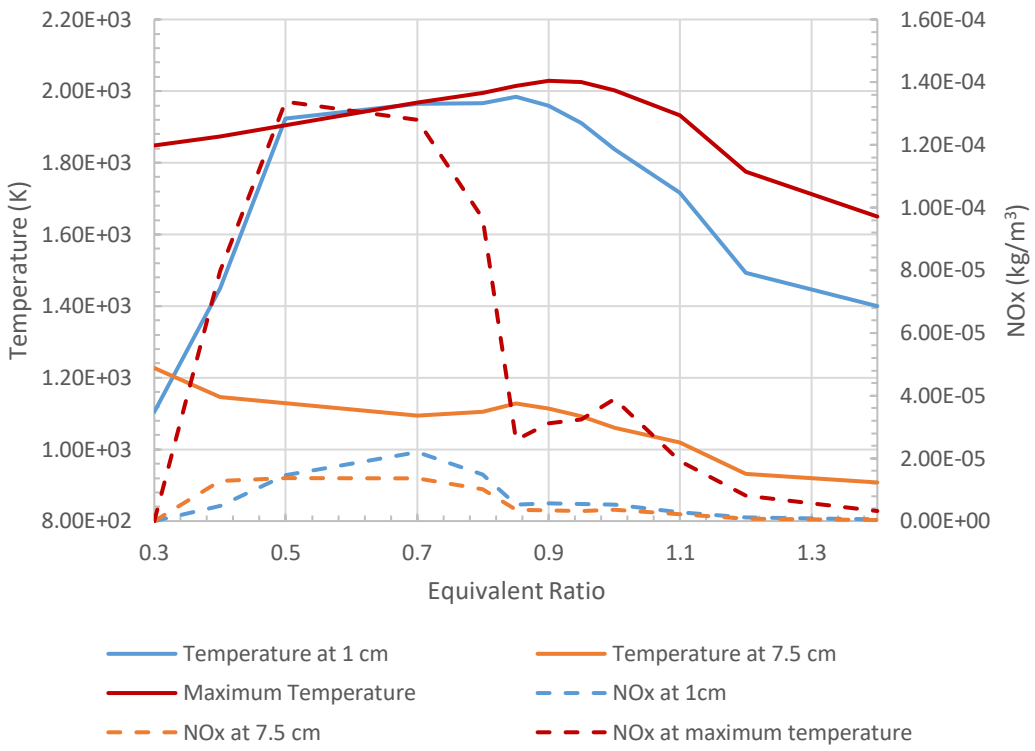

Figure 40: Flame Temperature and NO_x emission

Flame temperature and size are relatively higher when equivalent ratio is between 0.3 and 1.1. NO_x presence is relatively lower when equivalent ratio is between 1.85 and 1.4.

Equivalent ratio with high temperature (>1800K): 0.5-1.1

Equivalent ratio with low NO_x emission (<3.9×10^{-5} kg/m^3): 0.85-1.4

Recommended equivalent ratio to get high temperature with low emission: 0.85-1.1

Equivalent ratio between 0.85-1.1 has a higher temperature with low NO_x emissions. Therefore, this range is recommended.

Equivalent Ratio	0.50	0.80	0.85	1.10	1.15	1.40
High Temperature	>1800K		Recommended			
Low NO_x Emission					<3.9×10^{-5} kg/m^3	

5. EMISSIONS FROM INDUSTRIAL BURNER

Combustors release several gasses. Then the emitted gasses disperse through the atmosphere. The hazardousness of emitted gas depends on the emission rate as well as the way they get dispersed. In this study, the emission rate of a 20kW industrial burner was considered. Then the dispersion of the gas, considering Colombo area was analysed.

Figure 41: Dissipation of smoke emitted from an industrial chimney
Source: Times Higher Education [49]

The effect of emissions depends on the way they get dissipated in the atmosphere. Emissions must be diluted below the permissible level before exposed by people. Dissipation depends on wind velocity, chimney height and exhaust temperature. Dissipation of emissions of a 20kW industrial biogas burner in Colombo area was analysed in this study.

5.1. Modelling of the burner

For this study, a 20kW burner was considered as a typical case and simulated. The combustion model which was validated in chapter 3 was used to simulate this burner.

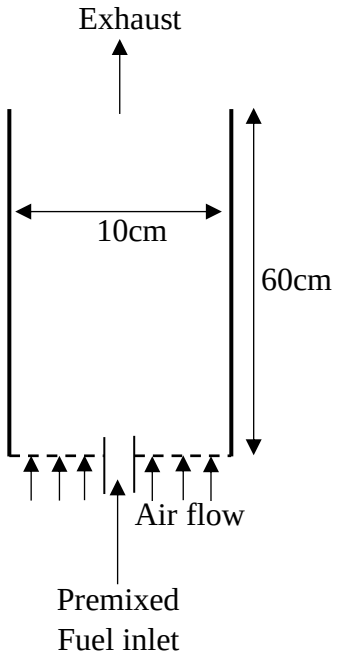

Figure 42: 20kW burner geometry

Table 11: Parameters of 20kW burner

Parameter	**Value**
Premixed fuel flow rate	0.0472m/s
Premixed equivalent ratio	1
Air co-flow	Natural draft
Wall	Adiabatic
Fuel inlet pressure	Zero gradient
Air inlet pressure	1 atm
Exhaust pressure	1 atm
Exhaust temperature	Zero gradient
Exhaust velocity	Zero gradient
Chamber diameter	10cm
Nozzle diameter	25mm
Simulated chamber height	60m

Exhaust gas compositions from a 20kW biogas burner obtained by simulation are illustrated in Table 12.

Table 12: Composition of Emissions

Component	Mass fraction
NO	1.243×10^{-03}
NO_2	9.211×10^{-06}
O_2	1.682×10^{-01}
N_2	7.506×10^{-01}
CO_2	3.014×10^{-02}
H_2O	4.600×10^{-02}
SO_2	3.744×10^{-03}

1253 ppm of NO_x is emitted according to the simulation, which compares well with the literature-based range of 100ppm to 1800ppm [37]. SO_2 emissions reach 3744 ppm and trace amounts of unburnt CH_4 and H_2S remain in the exhaust gas.

5.2. Atmospheric dispersion modelling

The environmental impact results mainly from NOx and SO_2. Therefore, stack emission as a point source was modelled and simulated to understand NOx and SO_2 spread in the atmosphere. The ground was assumed to be a flat terrain with a uniform roughness. The atmosphere was assumed as in neutral state. The vertical wind profile was obtained using power law (5.1) [38].

$$u = u_r \left(\frac{z}{z_r}\right)^{\frac{1}{7}} \tag{5.1}$$

CFD simulations were performed for 5m/s wind speed at 200m height above the ground level, which is the average wind speed in Colombo area [39], and for 1m/s.

The continuity equation for the conservation of mass is given in (5.2).

$$\frac{\partial \rho}{\partial t} + \nabla.(\rho u) = 0 \tag{5.2}$$

Generally, incompressibility is assumed in atmospheric flows modelling. Ignoring density variations reduces equation (5.2) to (5.3).

$$\nabla . u = 0 \tag{5.3}$$

Momentum conservation for an incompressible, Newtonian fluid (Navier–Stokes equations) is defined in equation (5.4).

$$\frac{\partial u}{\partial t} + (u.\nabla)u = -\frac{1}{\rho}\nabla p + \nu\nabla^2 u + \frac{1}{\rho}F \tag{5.4}$$

$$F = \rho g + F_c \tag{5.5}$$

Equation (10) implements the buoyancy force to the solver.

Navier–Stokes's equations are highly nonlinear and tend to divergence. The Boussinesq approximation reduces the nonlinearity and stabilizes the simulation [40]. Density is assumed to be vary linearly with temperature only as given in equation (5.6).

$$\rho = \rho_{0-}\rho_0\beta(T - T_0) \tag{5.6}$$

$$\frac{\partial u}{\partial t} + (u.\nabla)u = -\frac{1}{\rho_0}\nabla(p - \rho_0 g.z) + \nu\nabla^2 u - g\beta(T - T_0) + F_c \tag{5.7}$$

The Smagorinsky LES model was used to simulate turbulence [41]. Chimney height was assumed as 30m, which is within the environmental standards and mostly used in the area [42]. According to simulation results of the combustion chamber, gas velocity at the exhaust of the chimney is 0.5m/s. Exhaust temperature was assumed as 350 ˚C.

On a global scale, the Coriolis force contributes to circulation. Coriolis force can be expressed as (5.8).

$$F_c = -2m\omega V sin\varphi \tag{5.8}$$

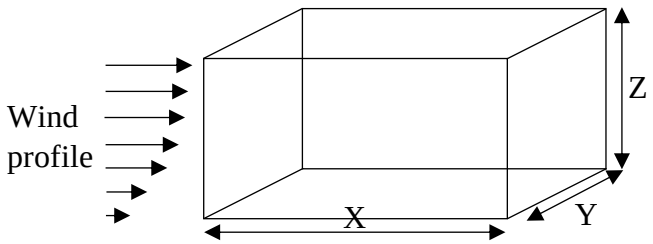

Figure 43: Geometry of domain

The simulation was done for a domain of a cuboid as in Figure 43.

5.2.1. Model Validation

Monin–Obukhov provides experimental data on atmospheric wind velocity profile [43]. Atmospheric model developed used to simulate a domain of 5000m×500m×500×m (Length×width×height) and compared the simulation results of

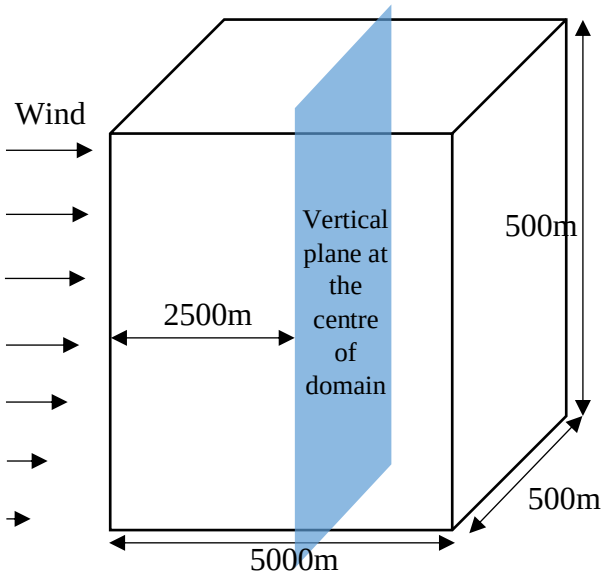

Figure 44: Geometry of the domain used to validate atmospheric wind model

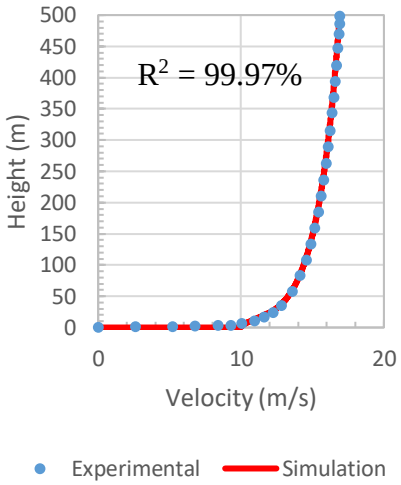

Figure 45: Wind velocity profile

a vertical plane at the centre of the domain with experimental data. Concluded that the wind profile is accurately simulated as the comparison with experimental data has a R^2 value above 99%.

Vu Tran et al [43] Has used experimental data of SF_6 dispersion to validate an atmospheric dispersion model. The same system was simulated with the developed model and compared experimental data with simulation results.

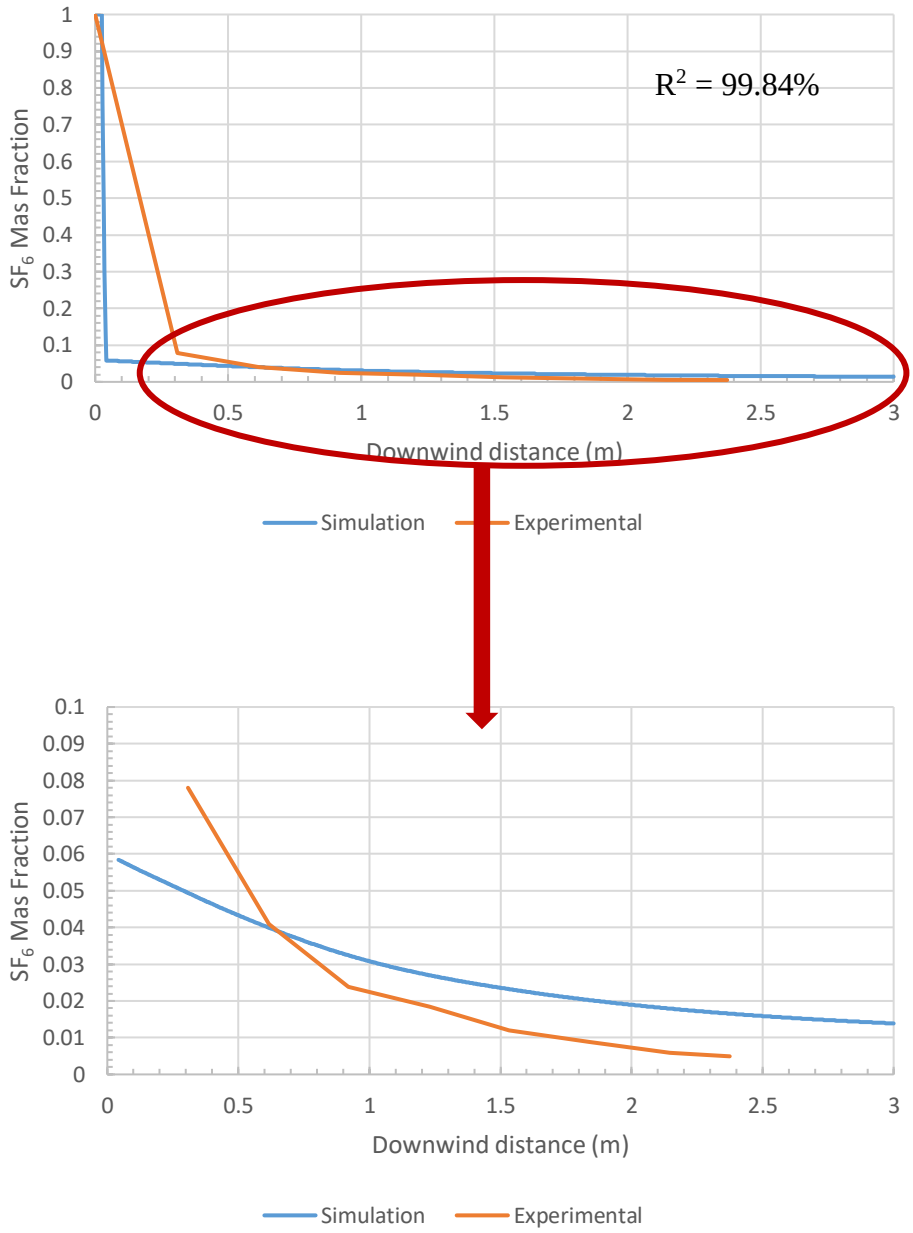

Figure 46: Comparison of SF_6 dispersion Experimental and Simulation data

The simulation results show model can be validated by comparing with experimental data as in Figure 46 (R^2 is above 99%). More accurate results can be achieved using dynamic Smagorinsky parameters [44]. This validated model was used to simulate emission dispersion from an industrial burner.

5.3. Emission

Combustion model which is validated above is used to simulate biogas combustion system. Exhaust gas compositions from a 20kW biogas burner are as in Table 13 according to simulation results.

Table 13: Composition of emissions

Component	Mass fraction
NO	1.243×10^{-03}
NO_2	9.211×10^{-06}
CH_4	1.285×10^{-17}
O_2	1.682×10^{-01}
N_2	7.506×10^{-01}
CO_2	3.014×10^{-02}
H_2O	4.600×10^{-02}
SO_2	3.744×10^{-03}

1253.04 ppm of NO_x is emitted according to the simulation. According to the literature, this can be varied from 100ppm to 1800ppm, which is complied with simulation results [37]. SO_2 emission is 3744.44 ppm and Trace amount of unburnt CH_4 and H_2S are remained in the exhaust gas.

5.3.1. Environmental levels

The maximum permissible level of NO_x in the Colombo area is 0.05ppm and SO_2 is 0.03ppm [45]. Exceeding 0.033ppm of annual mean NO_x and 0.016ppm of 24-hour mean SO_2 is considered as toxic [46]. Currently, the average concentration of NO_x is 0.02352ppm and of SO_2 is 0.00784ppm in Colombo area [47].

5.3.2. Pollutant dispersion simulations

The CFD simulations were conducted for point emissions at 30m height with wind speeds of 5m/s and 1m/s for the domain of Figure 47. Different mesh sizes were simulated to finalize the suitable mesh size and selected 150×10×30 cells for the domain as in Figure 47.

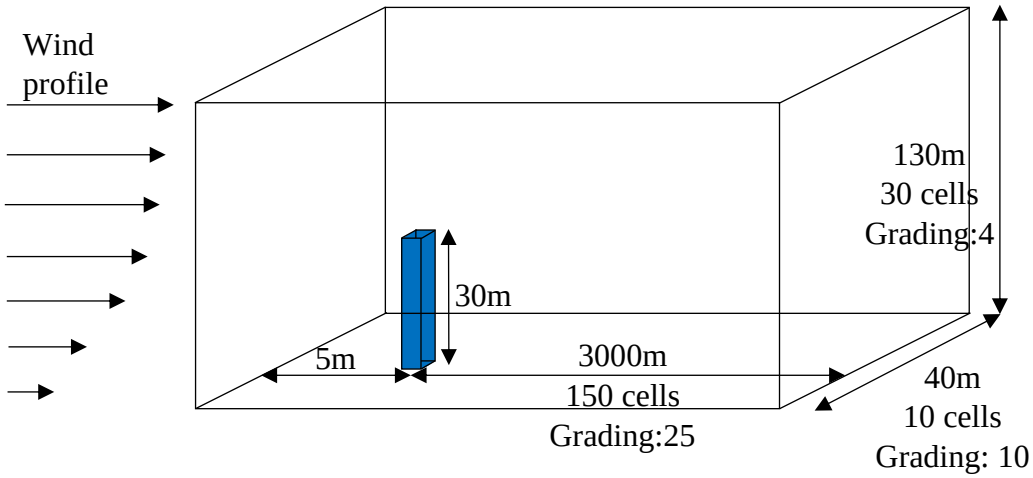

Figure 47: Geometry of the domain used to simulate atmospheric dispersion

Concentrations only in the downwind direction are presented as concentrations in other directions are negligible according to the simulation results. Figure 48 and Figure 49 show the area which exceeds 0.05ppm of NO_2 and 0.03ppm of SO_2 in the vertical plane in the downwind direction.

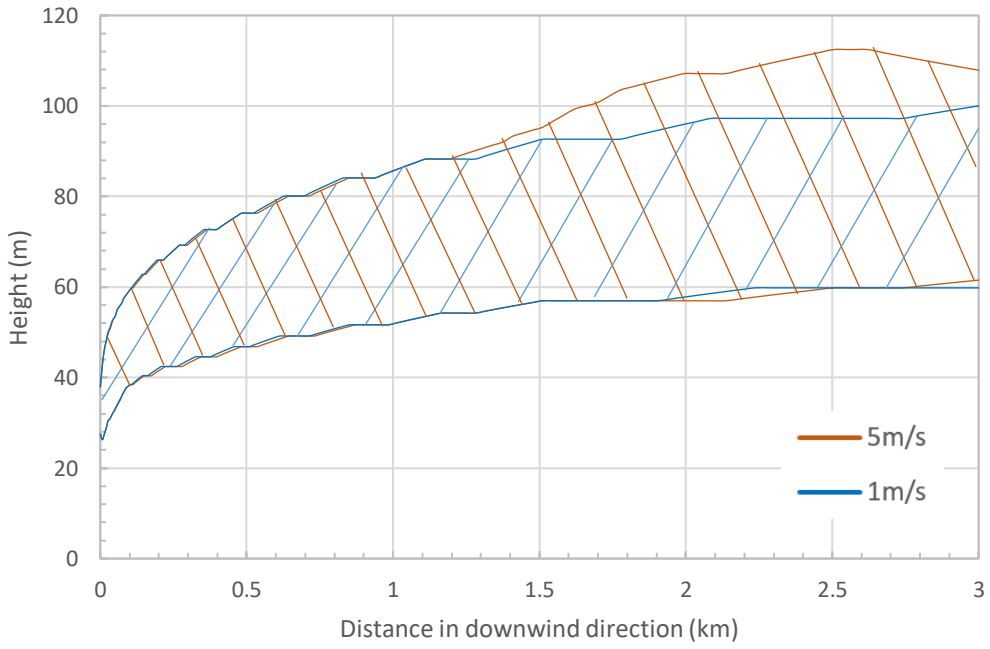

Figure 48: Height to the area that exceeds permissible level of NO_2

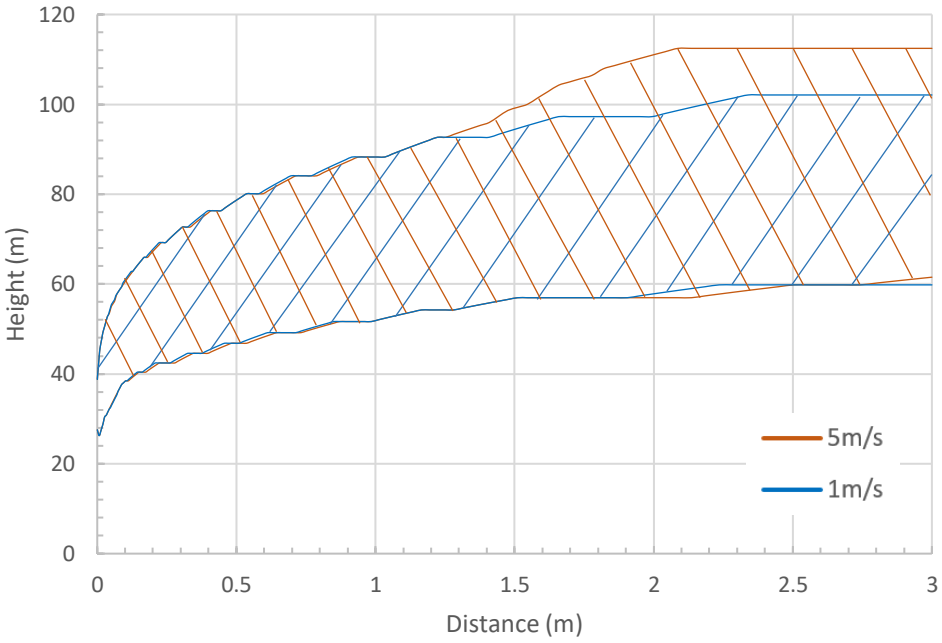

Figure 49: Height to the area that exceeds permissible level of SO_2

Ground level concentrations of emitted gasses relative to currently available concentrations are presented in Figure 50 and Figure 51.

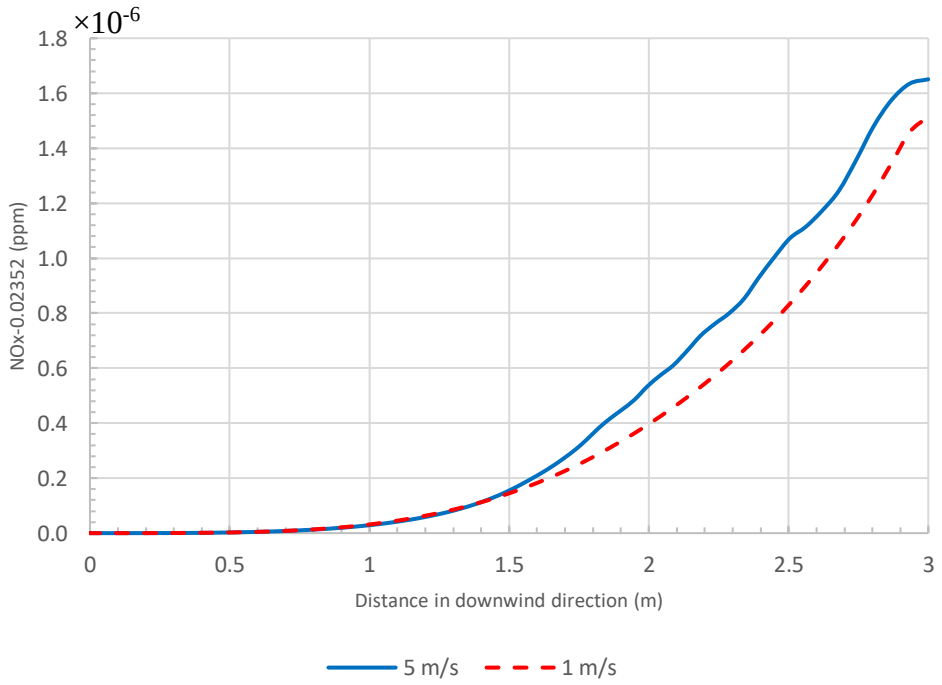

Figure 50: NO_2 concentration at ground level

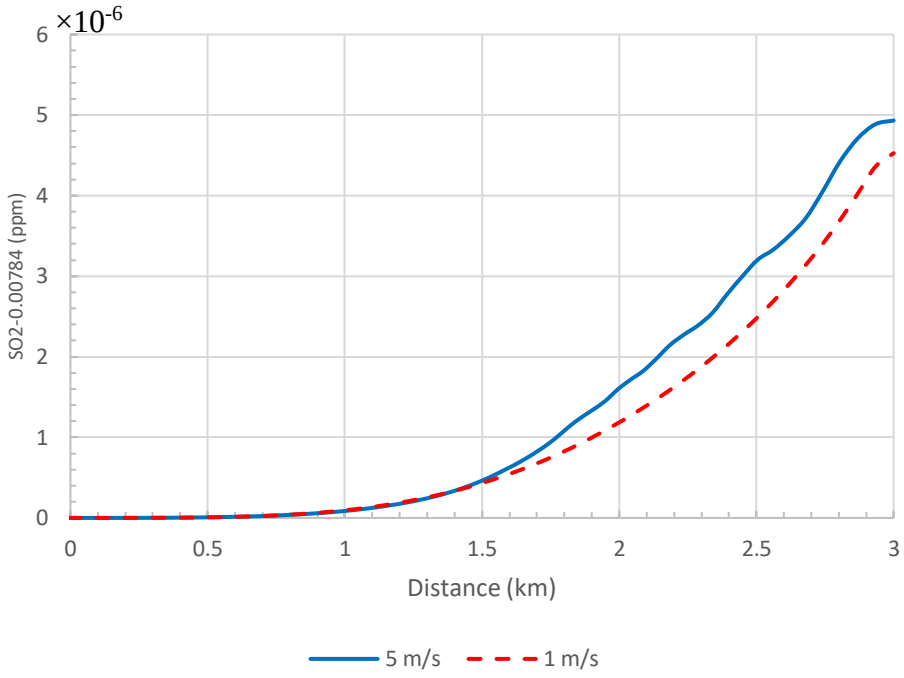

Figure 51: SO_2 concentration at ground level

6. CONCLUSION

Biogas is a highly available renewable fuel. It is released mainly from anaerobic digesters of industries. When they are used as a fuel, optimum conditions should be maintained to get maximum efficiency with less emissions. In this study optimum equivalent ratio in a biogas burner and dispersion of emissions in the atmosphere from an industrial burner is analysed.

CFD simulations can be used to get flame profile of a burner. Comparison of CFD results with experimental data validated that the results obtained by CFD simulations are accurate. The validated model is used to simulate combustion systems and atmospheric dispersion.

Simulations of a small-scale combustion chamber shows that rich combustion gives a high temperature flame. But it releases a large amount of NO_x. 0.5-1.1 Equivalent ratio range has the highest temperature in the considered combustion chamber. Lean combustion releases less NOx but gives a low temperature flame. 0.85-1.4 Equivalent ratio range release a low amount of NOx. Therefore, maintaining an equivalent ratio between 0.85-1.1 is recommended for the considered system.

Atmospheric dispersion of emissions from a 20kW industrial burner was analysed. Because of the exhaust velocity and high exhaust temperature, emitted gasses move upward (from the ground). They get more widely dispersed with higher wind velocities (Figure 48 and Figure 49) due to additional turbulence. Therefore, ground level concentrations tend to be higher with greater wind speeds as shown in Figure 50 and Figure 51.

The permissible levels of emitted gasses exceed in the atmosphere above height of 30m. The gases do not get diluted below permissible levels within 3km in the downwind direction in the atmosphere. However, ground level concentrations do not exceed permissible levels within the considered distance.

The developed computational fluid dynamic models in this study can be used to simulate and analyse any biogas combustion system and emission dispersion in the atmosphere.

References

[1] A. H. Igoni, M. J. Ayotamuno, C. L. Eze, S. O. T. Ogaji and S. Probert, "Designs of anaerobic digesters for producing biogas from municipal solid-waste," *Applied Energy,* vol. 85, no. 6, pp. 430-438, 2008.

[2] A. Jaffrin, N. Bentounes, A. M. Joan and S. Makhlouf, "Landfill Biogas for heating Greenhouses and providing Carbon Dioxide Supplement for Plant Growth," *Biosystems Engineering,* vol. 86, no. 1, pp. 113-123, 2003.

[3] J. Durkee, "US and global environmental regulations," in *Management of Industrial Cleaning Technology and Processes*, Elsevier Science, 2006, pp. 43-98.

[4] M. Shao, Y. Zhang, L. Zeng, X. Tang, J. Zhang, L. Zhong and B. Wang, "Ground-level ozone in the Pearl River Delta and the roles of VOC and NOx in its production," *Journal of Environmental Management,* vol. 90, no. 1, pp. 512-518, 2009.

[5] N. Imanaka and T. Masui, "Advances in direct NOx decomposition catalysts," *Applied Catalysis A: General,* vol. 431–432, no. 26, pp. 1-8, 2012.

[6] J. S. Pandey, R. Kumar and S. Devotta, "Health risks of NO2, SPM and SO2 in Delhi (India)," *Atmospheric Environment,* vol. 39, no. 36, pp. 6868-6874, 2005.

[7] J.-Y. Chen, "Proceedings of the Third International Workshop on Measurement and Computation of Turbulent Nonpremixed Flames," Colorado, 1998.

[8] Pooja Ghosh, Goldy Shah, Shivali Sahota, Lakhveer Singh, Virendra Kumar Vijay, "Biogas production from waste: technical overview," in *Bioreactors,*, New Delhi, Elsevier, 2020, pp. 89-104.

[9] "Biogas composition," 2009. [Online]. Available: www.biogas-renewable-energy.info/biogas_composition.html.

[10] C. T. Bowman, "Gas-Phase Reaction Mechanisms for Nitrogen Oxide Formation and Removal in Combustion," *Pollutants from Combustion. NATO Science Series (Series C: Mathematical and Physical Sciences),* vol. 547, no. 1, pp. 123-144, 2000.

[11] C. P. Fenimore, "Formation of nitric oxide in premixed hydrocarbon flames," *Symposium (International) on Combustion,* vol. 13, no. 1, pp. 373-380, 1971.

[12] "Burner Optimisation for NOx Control (Excess Air Control, Burner Fine Tuning)," 20 January 2018. [Online]. Available: https://www.iea-coal.org/burner-optimisation-for-nox-control-excess-air-control-burner-fine-tuning/.

[13] Seik Park, Gyung Min Choi, MamoruTanahashi, "Demonstration of a gas turbine combustion-tuning method and sensitivity analysis of the combustion-tuning parameters with regard to NOx emissions," *Fuel*, pp. 1134-1142, 2019.

[14] Hartmut Spliethoff, Ulrich Greul, Helmut Rüdiger, Klaus R.G.Hein, "Basic effects on NOx emissions in air staging and reburning at a bench-scale test facility," *Fuel*, pp. 560-564, April 1996.

[15] T. N. Roger Salzmann, "Fuel Staging for NOx Reduction in Biomass Combustion: Experiments and Modeling," *Energy & Fuels*, pp. 575-582, 11 April 2001.

[16] João Baltasar, Maria G. Carvalho, Pedro Coelho, MárioCosta, "Flue gas recirculation in a gas-fired laboratory furnace: Measurements and modelling," *Fuel*, pp. 919-929, August 1997.

[17] Feng Zhou, Jianqin Fu, Denghui Li, Jingping Liu, Chia-fon F. Lee, Yanshan Yin,, "Experimental study on combustion, emissions and thermal balance of high compression ratio engine fueled with liquefied methane gas," *Applied Thermal Engineering*, vol. 161, no. 1, pp. 1-14, 2019.

[18] Wen Zeng, , Jing Liu, Hongan Ma, Yu Liu, Aiguo Liu, "Experimental study on the flame propagation and laminar combustion," *Energy*, vol. 158, no. 1, pp. 437-448, 2018.

[19] Peter H. Joo, Marc R.J. Charest, Clinton P.T. Groth, Ömer L. Gülder, "Comparison of structures of laminar methane–oxygen and methane–air," *Combustion and Flame*, vol. 160, no. 1, pp. 1990-1998, 2013.

[20] Tongchit Suthisripok, Thananchai Promjun, Assawin Rangron, "A Comparative Study of a used 4-Stroke Motorcycle Engine Performance," *The 7th International Conference on Automotive Engineering*, vol. 28, no. 1, pp. 47-55, 2011.

[21] H.S. Zhen a, C.W. Leung, C.S. Cheung, Z.H. Huang, "Characterization of biogas-hydrogen premixed," *International Journal of Hydrogen Energy*, vol. 39, no. 25, pp. 13292-13299, 2014.

[22] Maruntalu O, Lazaroiu G, Bondrea D A, "Mathematical model for air pollutant dispersion emitted by fuel combustion," *UPB Scientific Bulletin*, vol. 77, no. 4, p. 229–236, 2015.

[23] H. Whaley, “A proposed canadian standard for estimating atmospheric dispersion of combustion source pollution from chimneys,” *Atmospheric Environment (1967),* vol. 3, no. 2, pp. 177-195, 1969.

[24] F. Toja-Silva, J. Chen, S. Hachinger and F. Hase, “CFD simulation of CO2 dispersion from urban thermal power plant: Analysis of turbulent Schmidt number and comparison with Gaussian plume model and measurements,” *Journal of Wind Engineering and Industrial Aerodynamics,* vol. 169, pp. 177-193, 2017.

[25] Gregory P. Smith, David M. Golden, Michael Frenklach, Nigel W. Moriarty, Boris Eiteneer, Mikhail Goldenberg, C. Thomas Bowman, Ronald K. Hanson, Soonho Song, William C. Gardiner, Jr., Vitali V. Lissianski, Zhiwei Q, “GRI-Mech 3.0,” [Online]. Available: http://combustion.berkeley.edu/gri-mech/version30/text30.html. [Accessed 2021].

[26] H. Selim, A. K. Gupta and M. Sassi, “Reduced Mechanism for Hydrogen Sulfide Oxidation,” *Proceedings of the ASME 2009 International Design Engineering Technical Conferences and Computers and Information in Engineering Conference,* vol. 2, pp. 263-278, 2009.

[27] Francesco Contino, Jean-Baptiste Masurier, Fabrice Foucher, Tommaso Lucchinid, Gianluca D’Errico, Philippe Dagaut, “CFD simulations using the TDAC method to model iso-octane combustion for a large range of ozone seeding and temperature conditions in a single cylinder HCCI engine,” *Fuel,* pp. 179-184, 2014.

[28] Zhiyi Li, Michał T. Lewandowski, Francesco Contino, Alessandro Parente, “Assessment of On-the-Fly Chemistry Reduction and Tabulation Approaches for the Simulation of Moderate or Intense Low-Oxygen Dilution Combustion,” *Energy & Fuels,* vol. 32, no. 10, pp. 10121-10131, 2018.

[29] Parviz Moin, Krishnan Mahesh, “Direct Numerical Simulation: A Tool in Turbulence Research,” *Annual Review of Fluid Mechanics,* vol. 30, no. 1, pp. 539-578, 1998.

[30] Heinz Pitsch, “Large-Eddy Simulation of Turbulent Combustion,” *Annual Review of Fluid Mechanics,* vol. 38, no. 1, pp. 453-482, 2006.

[31] Svetlana V. Poroseva, Juan D. Colmenares, Scott M. Murman, “On the accuracy of RANS simulations with DNS data,” *Physics of Fluids,* vol. 28, no. 1, pp. 1-21, 2016.

[32] Masoud Darbandi, Mehdi Zakyani, Gerry Schneider, "Evaluation of Different k-omega and k-epsilon Turbulence Models in a New Curvilinear Formulation," in *17th AIAA Computational Fluid Dynamics Conference*, Toronto, 2012.

[33] M. Herout, J. Malaťák, L. Kučera and T. Dlabaja, "Biogas composition depending on the type of plant biomass used," *Research in Agricultural Engineering,* vol. 57, no. 4, pp. 137-143, 2011.

[34] S. Rasi, A. Veijanen and J. Rintala, "Trace compounds of biogas from different biogas production plants," *Energy,* vol. 32, no. 8, pp. 1375-1380, 2007.

[35] B. Bharathiraja, T. Sudharsana, J. Jayamuthunagai, R. Praveenkumar, S. Chozhavendhan and J. Iyyappan, "Biogas production–A review on composition, fuel properties, feed stock and principles of anaerobic digestion," *Renewable and Sustainable Energy Reviews,* vol. 90, pp. 570-582, 2018.

[36] N. W. Ryan, M. M. Johnson, "Transistion from laminar to turbulent flow in pipes," *A.1.Ch.E. Journal,* vol. 5, no. 4, pp. 433-435, 1959.

[37] M. Talibi, P. Hellier and N. Ladommatos, "Combustion and exhaust emission characteristics, and in-cylinder gas composition, of hydrogen enriched biogas mixtures in a diesel engine," *Energy*, vol. 124, no. 1, pp. 397-412, 2017.

[38] S. A. Hsu, E. A. Meindl and D. B. Gilhousen, "Determining the Power-Law Wind-Profile Exponent under Near-Neutral Stability Conditions at Sea," *Journal of Applied Meteorology and Climatology,* vol. 33, no. 6, p. 757–765, 1994.

[39] "Global Wind Atlas," Technical University of Denmark, 2019. [Online]. Available: https://globalwindatlas.info/. [Accessed 2021].

[40] F. Porté-Agel, Y.-T. Wu, H. Lu and R. J. Conzemius, "Large-eddy simulation of atmospheric boundary layer flow through wind turbines and wind farms," *Journal of Wind Engineering and Industrial Aerodynamics,* vol. 99, no. 4, pp. 154-168, 2011.

[41] M. Rösler, V. John and N. Ahmed, "The Smagorinsky turbulence model," Bachelor thesis at the Institute of Mathematics of Freie University, Berlin, 2015.

[42] Central Environmental Authority - Sri Lanka, "Gazette Extraordinary of The Democratic Socialist Republic of Sri Lanka, No. 2126/36," 2019.

[43] Vu Tran, E. Y. K. Ng, Martin Skote, "CFD simulation of dense gas dispersion in neutral atmospheric boundary layer with OpenFOAM," *Meteorology and Atmospheric Physics,* vol. 132, no. 1, p. 273–285, 2020.

[44] E. S. Ferreira Jr, S. S. V. Vianna, “Large Eddy Simulation combined with equivalent diameter for turbulent jet modelling and,” *Brazilian Congress of Chemical Engineering,* vol. 33, no. 3, pp. 525-540, 2016.

[45] Ministry of Environment and Natural Resources, “Gazette Extraordinary of the Democratic Socialist Republic of Sri Lanka, No. 1562/22,” 2008.

[46] World Health Organization , “WHO Air quality guidelinesfor particulate matter,ozone, nitrogendioxide and sulfur dioxide - Global update 2005 - Summary of risk assessment,” 2005.

[47] “Air quality and pollen forecast for Colombo,” meteoblue , 9 3 2021. [Online]. Available: https://www.meteoblue.com/en/weather/outdoorsports/airquality/colombo_sri-lanka_1248991. [Accessed 9 3 2021].

[48] J. Rajika and M. Narayana, “Modelling and simulation of wood chip combustion in a hot air generator system,” *SpringerPlus,* vol. 5, no. 1, pp. 1-19, 2016.

[49] J. Grove, “Nobel wins show basic research 'key to climate battle',” Times Higher Education, 11 10 2021. [Online]. Available: https://www.timeshighereducation.com/news/nobel-wins-show-basic-research-key-climate-battle. [Accessed 15 10 2021].

APPENDIX

Appendix A: Modified OpenFOAM Code with wall heat loss

OpenFOAM version: dev (2020 March)

Source code:

buoyantReactingFoam.C

```
/*---------------------------------------------------------------------------*\
  =========                 |
  \\      /  F ield         | OpenFOAM: The Open Source CFD Toolbox
   \\    /   O peration     | Website:  https://openfoam.org
    \\  /    A nd           | Copyright (C) 2012-2021 OpenFOAM Foundation
     \\/     M anipulation  |
-------------------------------------------------------------------------------
License
    This file is part of OpenFOAM.

    OpenFOAM is free software: you can redistribute it and/or modify it
    under the terms of the GNU General Public License as published by
    the Free Software Foundation, either version 3 of the License, or
    (at your option) any later version.

    OpenFOAM is distributed in the hope that it will be useful, but WITHOUT
    ANY WARRANTY; without even the implied warranty of MERCHANTABILITY or
    FITNESS FOR A PARTICULAR PURPOSE.  See the GNU General Public License
    for more details.

    You should have received a copy of the GNU General Public License
    along with OpenFOAM.  If not, see <http://www.gnu.org/licenses/>.

Application
    buoyantReactingFoam

Description
    Transient solver for turbulent flow of compressible reacting fluids with
    enhanced buoyancy treatment and optional mesh motion and mesh topology
    changes.

    Uses the flexible PIMPLE (PISO-SIMPLE) solution for time-resolved and
    pseudo-transient simulations.

\*---------------------------------------------------------------------------*/

#include "fvCFD.H"
#include "dynamicFvMesh.H"
#include "fluidReactionThermo.H"
#include "combustionModel.H"
#include "dynamicMomentumTransportModel.H"
#include "fluidReactionThermophysicalTransportModel.H"
#include "multivariateScheme.H"
#include "pimpleControl.H"
#include "pressureReference.H"
#include "hydrostaticInitialisation.H"
#include "CorrectPhi.H"
#include "fvModels.H"
#include "fvConstraints.H"
#include "localEulerDdtScheme.H"
#include "fvcSmooth.H"

// * * * * * * * * * * * * * * * * * * * * * * * * * * * * * * * * * * * * * //
```

```
int main(int argc, char *argv[])
{
    #include "postProcess.H"

    #include "setRootCaseLists.H"
    #include "createTime.H"
    #include "createDynamicFvMesh.H"
    #include "createDyMControls.H"
    #include "initContinuityErrs.H"
    #include "createFields.H"
    #include "createFieldRefs.H"
    #include "createRhoUfIfPresent.H"

    turbulence->validate();

    if (!LTS)
    {
        #include "compressibleCourantNo.H"
        #include "setInitialDeltaT.H"
    }

    // * * * * * * * * * * * * * * * * * * * * * * * * * * * * * * * * * * * * //

    Info<< "\nStarting time loop\n" << endl;

    IOdictionary thermophysicalProperties
    (
        IOobject
        (
            "thermophysicalProperties",
            runTime.constant(),
            mesh,
            IOobject::MUST_READ,
            IOobject::NO_WRITE
        )
    );
    dimensionedScalar k
    (
        thermophysicalProperties.lookup("k")
    );
    dimensionedScalar h
    (
        thermophysicalProperties.lookup("h")
    );
    string ptname
    (
        thermophysicalProperties.lookup("wall")
    );

    label patchID=mesh.boundaryMesh().findPatchID(ptname);
    const polyPatch& wallPatch =mesh.boundaryMesh()[patchID];

    while (pimple.run(runTime))
    {
        #include "readDyMControls.H"

        // Store divrhoU from the previous mesh so that it can be mapped
        // and used in correctPhi to ensure the corrected phi has the
        // same divergence
        autoPtr<volScalarField> divrhoU;
        if (correctPhi)
        {
            divrhoU = new volScalarField
            (
                "divrhoU",
                fvc::div(fvc::absolute(phi, rho, U))
            );
        }

        if (LTS)
        {
            #include "setRDeltaT.H"
```

```
}
else
{
    #include "compressibleCourantNo.H"
    #include "setDeltaT.H"
}

runTime++;

Info<< "Time = " << runTime.timeName() << nl << endl;

// --- Pressure-velocity PIMPLE corrector loop
while (pimple.loop())
{
    if (!pimple.flow())
    {
        if (pimple.models())
        {
            fvModels.correct();
        }

        if (pimple.thermophysics())
        {
            #include "YEqn.H"
            #include "EEqn.H"
        }
    }
    else
    {
        if (pimple.firstPimpleIter() || moveMeshOuterCorrectors)
        {
            // Store momentum to set rhoUf for introduced faces.
            autoPtr<volVectorField> rhoU;
            if (rhoUf.valid())
            {
                rhoU = new volVectorField("rhoU", rho*U);
            }

            fvModels.preUpdateMesh();

            // Do any mesh changes
            mesh.update();

            if (mesh.changing())
            {
                gh = (g & mesh.C()) - ghRef;
                ghf = (g & mesh.Cf()) - ghRef;

                MRF.update();

                if (correctPhi)
                {
                    #include "correctPhi.H"
                }

                if (checkMeshCourantNo)
                {
                    #include "meshCourantNo.H"
                }
            }
        }

        if (pimple.firstPimpleIter() && !pimple.simpleRho())
        {
            #include "rhoEqn.H"
        }

        if (pimple.models())
        {
            fvModels.correct();
        }
```

```
                #include "UEqn.H"

                if (pimple.thermophysics())
                {
                    #include "YEqn.H"
                    #include "EEqn.H"
                }

                // --- Pressure corrector loop
                while (pimple.correct())
                {
                    #include "pEqn.H"
                }

                if (pimple.turbCorr())
                {
                    turbulence->correct();
                    thermophysicalTransport->correct();
                }
            }
        }

        forAll(wallPatch,faceI)
        {


            vector pos0(mesh.points()[wallPatch[faceI][0]]);
            vector pos2(mesh.points()[wallPatch[faceI][2]]);


            scalar r1=pos0[0];
            scalar L=pos2[2]-pos0[2];
            scalar Tw=thermo.T().boundaryFieldRef()[patchID][faceI];
            scalar Tr=373;
            scalar thickness=0.002;
            scalar r2=r1+thickness;
            scalar arcLength=pos2[1]-pos0[1];
            scalar R=pos2[0]-pos0[0];


            if(L==0)
            {
              dimensioned<double> Q_Loss=(Tw-
Tr)/((1/(k*R*arcLength/thickness))+(1/(h*R*arcLength)));
                    thermo.he().boundaryFieldRef()[patchID][faceI]-=Q_Loss.value();
            }
            else
            {
                     dimensioned<double> Q_Loss=(Tw-
Tr)/((std::log(r2/r1)/(L*k*(arcLength/r1)))+(1/h*L*(arcLength)));
                    thermo.he().boundaryFieldRef()[patchID][faceI]-=Q_Loss.value();
            }
        }

        rho = thermo.rho();

        runTime.write();

        Info<< "ExecutionTime = " << runTime.elapsedCpuTime() << " s"
            << "  ClockTime = " << runTime.elapsedClockTime() << " s"
            << nl << endl;
    }

    Info<< "End\n" << endl;

    return 0;
}
// ************************************************************************* //
```

Case files:

thermophysicalProperties

```
/*--------------------------------*- C++ -*----------------------------------*\
  =========                 |
  \\      /  F ield         | OpenFOAM: The Open Source CFD Toolbox
   \\    /   O peration     | Website:  https://openfoam.org
    \\  /    A nd           | Version:  dev
     \\/     M anipulation  |
\*---------------------------------------------------------------------------*/
FoamFile
{
    version     2.0;
    format      ascii;
    class       dictionary;
    location    "constant";
    object      thermophysicalProperties;
}
// * * * * * * * * * * * * * * * * * * * * * * * * * * * * * * * * * * * * * //

thermoType
{
    type            hePsiThermo;
    mixture         multiComponentMixture;
    transport       sutherland;
    thermo          janaf;
    energy          sensibleEnthalpy;
    equationOfState perfectGas;
    specie          specie;
}

defaultSpecie N2;
wall      "wall2";
fuel        CH4;

k         k [1 1 -3 -1 0 0 0] 14.4; //Source =
https://www.engineeringtoolbox.com/thermal-conductivity-metals-d_858.html
h         h [1 1 -3 -1 0 0 0] 50000;
#include "speciesThermo"

// ************************************************************************* //
```

Appendix B: Numerical schemes and Solution algorithms of DLR Flame simulation

Table 14: Numerical schemes of DLR flame

Time schemes		localEuler
Gradient schemes		Gauss linear
Divergence schemes	div(phi,U)	Gauss limitedLinearV 1
	div(phi,Yi)	Gauss limitedLinear01 1
	div(phi,h)	Gauss limitedLinear 1
	div(phi,K)	Gauss limitedLinear 1
	div(phid,p)	Gauss limitedLinear 1
	div(phi,epsilon)	Gauss limitedLinear01 1
	div(phi,Yi_h)	Gauss limitedLinear01 1
	div(phi,k)	Gauss limitedLinear01 1
	div(((rho*nuEff)*dev2(T(grad(U)))))	Gauss linear
Laplacian schemes		Gauss linear orthogonal
Interpolation schemes		linear
Surface normal gradient schemes		orthogonal

Table 15: Solution algorithms of DLR flame

	solver	preconditioner	tolerance	relTol
rho.*	diagonal			
GFinal	PCG	DIC	1e-5	0
p	PCG	DIC	1e-6	0.01
p_rgh	PCG	DIC	1e-6	0.01
pFinal	PCG	DIC	1e-6	0
p_rghFinal	PCG	DIC	1e-6	0
U,h,k,epsilon	PBiCGStab	DILU	1e-6	0.1
U,h,k,epsilonFinal	PBiCGStab	DILU	1e-6	0.1
Yi.*	PBiCG	DILU	1e-8	0.1

Appendix C: Numerical schemes and Solution algorithms of small-scale combustion chamber simulation

Table 16: Numerical schemes of small-scale combustion chamber

Time schemes		localEuler
Gradient schemes		Gauss linear
Divergence schemes	div(phi,U)	Gauss linearUpwind grad(U)
	div(phi,Yi)	Gauss limitedLinear01 1
	div(phi,h)	Gauss limitedLinear 1
	div(phi,K)	Gauss limitedLinear 1
	div(phid,p)	Gauss limitedLinear 1
	div(phi,epsilon)	bounded Gauss limitedLinear01 1
	div(phi,Yi_h)	Gauss limitedLinear01 1
	div(phi,k)	bounded Gauss limitedLinear01 1
	div(((rho*nuEff)*dev2(T(grad(U)))))	Gauss linear
Laplacian schemes		Gauss linear limited corrected 0.5
Interpolation schemes		linear
Surface normal gradient schemes		limited corrected 0.5

Table 17: Solution algorithms of small-scale combustion chamber

	solver	preconditioner	tolerance	relTol
rho.*	diagonal			
GFinal	PCG	DIC	1e-5	0
p	PCG	DIC	1e-6	0.01
p_rgh	PCG	DIC	1e-6	0.01
pFinal	PCG	DIC	1e-6	0
p_rghFinal	PCG	DIC	1e-6	0
U,h,k,epsilon	PBiCGStab	DILU	1e-6	0.1
U,h,k,epsilon Final	PBiCGStab	DILU	1e-6	0.1
Yi.*	PBiCG	DILU	1e-8	0.1

Appendix D: Biogas combustion simulator